

**Modeling the Potential for Large High-Severity Fires  
in the Klamath Basin Region of California and Oregon  
and Their Potential Impacts on Marten and Fisher**



Conservation Biology Institute

US Fish & Wildlife Service Cooperative Agreement # F18AC00504

Final Report, August 2019

## Table of Contents

<b>Introduction</b>	3
<b>Methods</b>	4
Modeling Exetent and Subregions	4
Fire and Environmental Predictor Data	6
Modeling Process	11
Model Evaluation	12
<b>Results</b>	13
High-severity Fire Risk Models	13
Potential Impacts of Severe Fire on Fisher and Marten Core and Linkage Habitats	22
<b>Data Products</b>	25
<b>Literature Cited</b>	26
<b>Appendices</b>	31
Appendix 1. Correlation matrix of predictors across entire study area	31
Appendix 2. Model response plots	32
Appendix 3. Black and white versions of figures.	45

## Introduction

The objective of this project was to use relatively recent fire severity data to create scientifically defensible maps of areas that may be at risk of high-severity fires in the Klamath region of northern California and southern Oregon over the next decade or so based on vegetation, terrain, and climate variables. As a first attempt of this nature for the region, the results should be interpreted with caution. Modeling fire risk is an inherently uncertain task given the stochastic nature of fire and how its effects are influenced by ignition timing and location, terrain, fuel conditions, and weather conditions and firefighter tactics during a fire. Many of these factors are not mapped or available for use in statistical analyses or predictive models, especially how real-time weather conditions and fire-fighting actions may have influenced fire behavior and ecological effects. Our intent was therefore to map the potential for large, severe fires based on available, landscape-scale, and longer-term data, not to predict real-time fire behavior nor to make precise predictions about future fires. Furthermore, at the time these models were prepared, climate data were not yet available at appropriate spatial resolution to correlate with fire severity data after the year 2010, which constrained our temporal window for model creation; and of course, climate and its effects on fire regimes are rapidly changing.

All of these issues add significant uncertainty to our landscape-scale predictions about where large severe fires are likely in the future. These results should therefore be considered preliminary and interpreted with appropriate caution as representing hypotheses about where severe fires *may* be more likely in the near future rather than as specific predictions about future fires. As better data become available, we urge improving on these models.

This effort complements CBI's effort to model habitat connectivity for forest species of concern in the region (Pacific marten and Pacific fisher)<sup>1</sup> by identifying important habitat core and connectivity areas that may be threatened by severe fires or forest management actions. The results of these preliminary fire-severity risk maps were overlaid onto modeled habitat and potential movement corridors for fisher and marten to map where habitat and population connectivity may be at greatest risk. The results can be used by USFWS in assessments of species' status and risks, and to help prioritize potential management interventions (e.g., fuels management), albeit with appropriate caution.

This is the first attempt we know of to prepare higher-resolution, statistically valid fire risk maps for this region. This information is needed because many USFWS Section 7 consultations involve fire and fuels management projects, and large high-severity fires can at least temporarily threaten population viability for at-risk species. The results can inform Strategic Habitat Conservation priorities of the Yreka USFWS Field Office and the greater Klamath Basin Demonstration Project.

---

<sup>1</sup> US Fish & Wildlife Service Cooperative Agreement # F17AC00856

## Methods

We statistically compared locations of high-severity fire patches from 1984 (when fire-severity mapping began) to 2010 (the most recent appropriately scaled climate data) to environmental variables likely to influence fire risks (vegetation, terrain, land-use, and climate variables). We used the potential predictive variables to create multivariate models of severe fire risk using the MaxEnt program (Phillips et al. 2006), training and testing models with randomly distributed points within large ( $\geq 1000$  ac) high-severity fire polygons from 1984-2010.

### Modeling Extent and Subregions

We modeled fire risks over the entire Klamath study area as well as in four subregions to better capture finer-scale regional patterns (Figure 1). We had planned to use ecological subsections to subdivide the study area, but they proved too small to provide adequate sample sizes of large, severe fires for statistical models. We therefore grouped ecological subsections or portions of subsections into four subregions based on ecological and climatic similarities, while maintaining adequate fire sample sizes within each.

Portions of the Northern California Coast and Northern California Coast Ranges were combined to create subregion 1a. This is the smallest subregion at 24,413 km<sup>2</sup> and has the lowest mean elevation (639 m; range -2 to 2458 m). It consists mostly of evergreen forest (52%) and shrub/scrub habitats (23%; Table 1). Its climate is strongly influenced by the Pacific Ocean, especially near the coast. Private landowners account for 62% of the area, followed by U.S. Forest Service (USFS), with 22%.

Subregion 1b, at 49,217 km<sup>2</sup>, comprises the entire Klamath Mountains ecoregional section as well as portions of Northern California Interior Coast Ranges and Oregon and Washington Coast Ranges. Elevation in this subregion ranges from -4 to 2746 m, with a mean of 767 m. It also consists mostly of evergreen forest (53%) and shrub/scrub vegetation (21%). The majority of the area is under private and USFS ownership (42 and 41% respectively).

Subregion 2 comprises the Southern Cascades ecoregional section combined with portions of Willamette Valley, Western Cascades, Sierra Nevada Foothills, and Sierra Nevada. This subregion has an area of 42,003 km<sup>2</sup> and has the largest elevation range (mean 1263 m, range 49 – 4304 m). Evergreen forest covers 67% of the area. USFS is the majority landowner, at 52%, with another 34% under private ownership.

Subregion 3 is the largest (58,173 km<sup>2</sup>), eastern-most, and highest-elevation (mean of 1532; range of 847 – 3003 m) subregion. It comprises the Modoc Plateau ecoregional section and portions of the Blue Mountain Foothills, Eastern Cascades, and Northwestern Basin and Range. This is the most inland of the subregions, with a generally warmer and drier climate, and is dominated by shrub/scrub vegetation (50%). Land ownership is a mix of USFS (31%), Bureau of Land Management (22%), and private (22%).

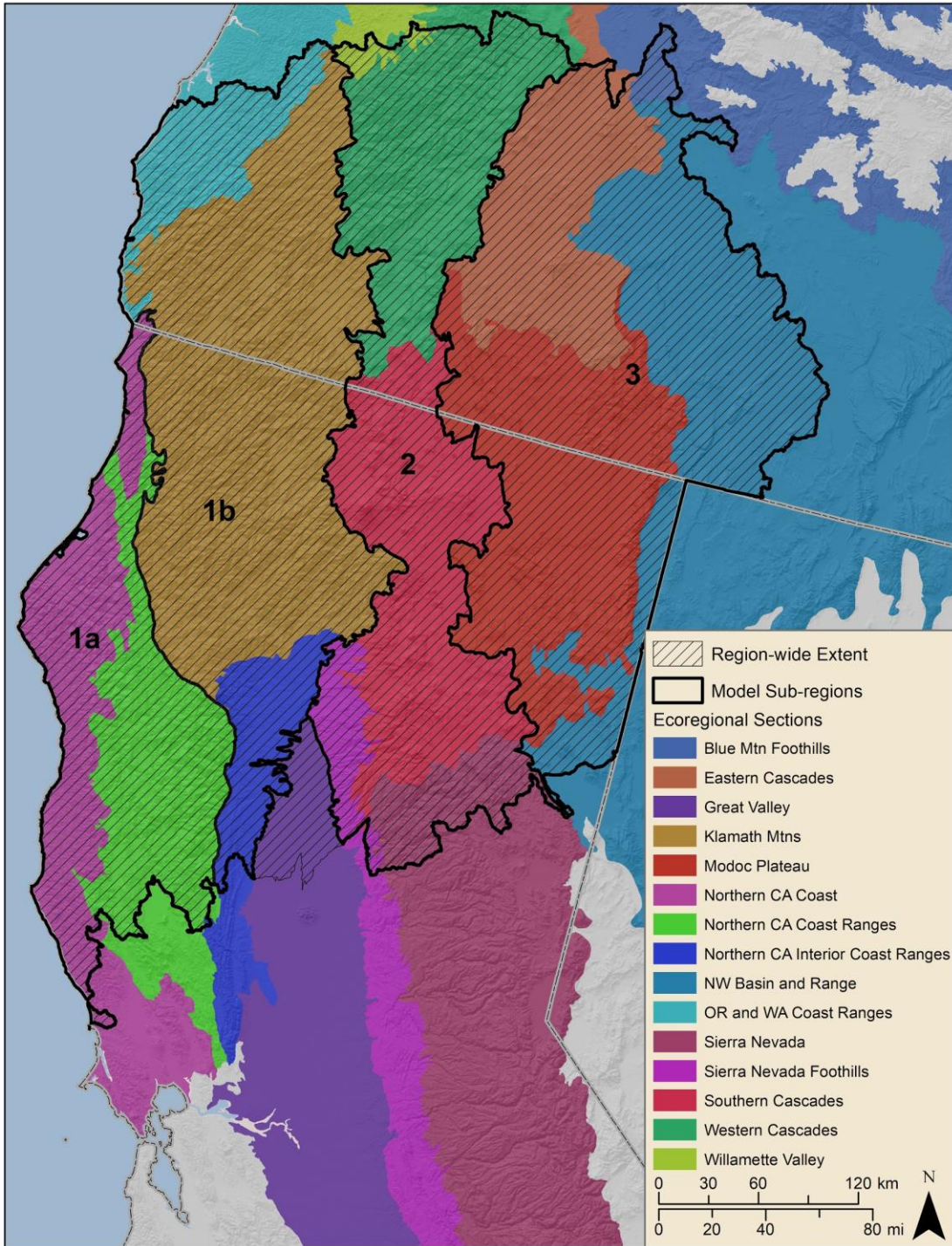


**Figure 1.** Region-wide extent and subregions based on ecological subsections.

**Table 1.** Land cover (percent) within each fire model subregion.

Land Cover Class	Subregion 1a	Subregion 1b	Subregion 2	Subregion 3
Open Water	0.58	0.74	1.17	2.65
Perennial Ice/Snow	0	0.04	0.03	0
Developed	3.94	4.06	1.17	1.17
Barren	0.35	0.52	1.45	2.82
Deciduous Forest	3.95	1.26	0.56	0.01
Evergreen Forest	51.68	53.23	67.20	26.44
Mixed Forest	7.51	4.64	0.35	0.03
Shrub/Scrub	22.51	21.22	17.60	49.75
Grassland/Herbaceous	7.54	10.09	8.05	9.11
Pasture/Hay, Cultivated Crops	1.42	3.45	2.03	5.68
Wetlands	0.52	0.75	0.39	2.34

### Fire and Environmental Predictor Data

We derived the response variable--high-severity fire occurrence within large (>1000 ac) fire perimeters--using the Monitoring Trends in Burn Severity database (MTBS, USDA Forest Service/U.S. Geological Survey, <https://mtbs.gov/>). Fire perimeter and severity data were used from 1984 to 2010 because 1984 is the earliest year available from MTBS, and 2010 was the most recent year for available climate normals data, which were important to training statistical models.

MTBS burn severity classes are derived from Landsat Thematic Mapper data by analyzing pre- and post-fire scenes to derive Differenced Normalized Burn Ratio (dNBR) data (Eidenshink et al. 2007). The continuous dNBR data are thresholded into burn severity classes (low, moderate, and high), with higher dNBR values correlated with higher burn severities. According to MTBS metadata, the burn severity classification thresholds are based on MTBS analysts' interpretation of dNBR data and also informed by ancillary data and known relationships between dNBR values and composite burn index (CBI) ground plot data (<https://www.mtbs.gov/mapping-methods>). Tracy et al. (2018) describe field characteristics of MTBS high and low severity classes from Schwind (2008), where high burn severity in forests results in  $\geq 75\%$  mortality of overstory trees, with long lasting overstory tree damage, and forest recovery taking up to several decades. Low burn severity impacts are

usually slight but may include up to 25% mortality in intermediate and large overstory trees, with recovery expected within 1-2 years.

From 1984-2010, there were 505 fires greater than 1,000 acres (404.7 ha) in the study region, of which 435 contained some high-severity burn areas. We generated a random sample of points within fire perimeters using the method developed by Davis et al. (2017): the number of random points generated within each fire perimeter was equal to the square root of the perimeter area divided by 40. We also forced a minimum distance of 500 m between the random points (based on testing of best distance in the northern Sierra Nevada - Southern Cascades; Syphard et al. 2018) to increase spatial independence and reduce spatial autocorrelation and model performance inflation (Veloz 2009, Boria et al. 2014). This process resulted in establishing 507 total sample points from within high-severity fire patches within the Klamath study area. We reserved 20% of those points for model evaluation, leaving a total of 406 points for model training, with a range in sample sizes per region from 47 in region 1a to 170 in region 1b (Figure 2, Table 2)<sup>2</sup>. We also generated an equal number of test points per region within low-severity burn areas to serve as ‘absences’ to enable us to calculate accuracy metrics for the models.

We assembled datasets of 30 potential predictor variables at 90-m resolution characterizing ignition sources (because a fire must occur before it can spread and develop into a large, high-severity burn) and direct and indirect drivers of fire, such as climate, topography, land use, and vegetation (Table 3). This resolution was selected as a compromise between coarser resolution climate predictors (1-km) and finer resolution vegetation and topographic predictors (30-m). We did not explicitly include fire history data as a potential predictor, in part because this would create temporal mismatches with climate, vegetation, and other variables without deriving layers for each of 26 years for the 1984-2010 time period and creating appropriate variables, which was beyond the scope of this project. Appropriate use of fire history data as a predictor should be considered in future updates to these models.

**Table 2.** Sample sizes of severe-fire training and testing points by model subregion<sup>2</sup>.

	Region-wide	Subregion 1a	Subregion 1b	Subregion 2	Subregion 3
Training	406	47	170	115	73
Testing	101	12	42	29	18

<sup>2</sup> Maxent has been shown to perform well at sample sizes as small as 5-10 occurrence points (Hernandez et al. 2006; Pearson et al. 2007; Wisz et al. 2008).

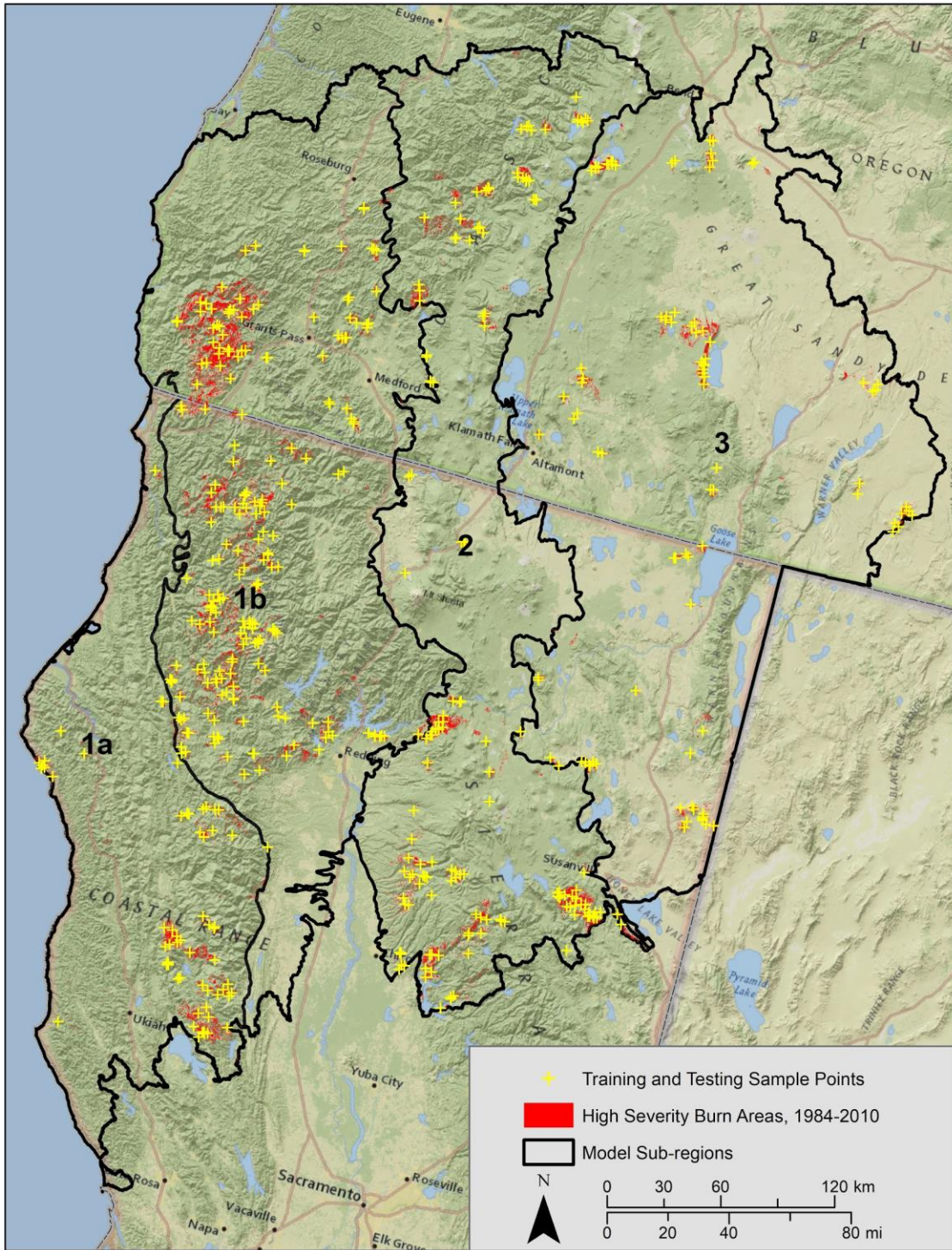


**Figure 2.** Sample points within high-severity portions of large (>1000 ac) fires from 1984-2010 used to train and test models.

**Table 3.** Potential predictor variables considered for inclusion in Klamath fire models.

Type	Predictor	Time Period	Source
Climate	July Maximum Vapor Pressure Deficit (VPD)	1981-2010	PRISM
Climate	Annual Maximum VPD	1981-2010	PRISM
Climate	Mean Temp Warmest Month (MWMT)	1981-2010	AdaptWest
Climate	Mean Temp Coldest Month (MTCM)	1981-2010	AdaptWest
Climate	Difference between MCMT and MWMT	1981-2010	AdaptWest
Climate	Mean Annual Precipitation	1981-2010	AdaptWest
Climate	Mean Summer Precipitation	1981-2010	AdaptWest
Climate	Precipitation as Snow	1981-2010	AdaptWest
Climate	Hargreave's Climatic Moisture Index	1981-2010	AdaptWest
Climate	Summer Heat Moisture Index	1981-2010	AdaptWest
Climate	Annual Heat Moisture Index	1981-2010	AdaptWest
Climate	Mean Annual Relative Humidity	1981-2010	AdaptWest
Climate	Actual Evapotranspiration	1981-2009	AdaptWest
Climate	Climatic Water Deficit	1981-2009	AdaptWest
Climate	Average Wind Power Density Class		NREL
Land Use	Distance to Primary/Secondary Roads		Open Street Map
Land Use	Distance to Major Roads		Open Street Map
Land Use	Distance to Major/Minor Roads		Open Street Map
Land Use	Distance to All Roads		Open Street Map
Land Use	Distance to Public Lands		PAD
Land Use	Housing Density	2010	TIGER
Land Use	Population Density	2010	TIGER
Land Use	Distance to Development	2010	NLCD Land Cover
Topography	Elevation		LANDFIRE
Topography	Slope		LANDFIRE
Topography	Solar Insolation Index ( $2 - (\sin((\text{slope}/90)180)) * (\cos(22 - \text{aspect}) + 1)$ ), Gustafson et al. 2003		CBI/LANDFIRE
Topography	Southwestness (transformed slope aspect $(\cos(\text{aspect}-255))$ ), Franklin 2003		CBI/LANDFIRE
Topography	Topographic Heterogeneity (standard deviation elevation calculated for center cell and three cell (90m) radius immediately surrounding)		NatureServe
Topography	Topographic Wetness Index (function of slope and upstream catchment area, calculated with SAGA GIS module)		CBI/LANDFIRE
Vegetation	Vegetation Type	2010	NLCD Land Cover

Several variables were tested to capture ignition susceptibility, both anthropogenic and natural (lightning). Anthropogenic factors also influence the likelihood of a fire growing and developing into a large, high-severity fire, because fires closer to human population centers and roads are more likely to be detected and accessible for suppression and control. We tested housing density, population density, proximity to roads, proximity to development, and proximity to public land, which all have been found to be associated with human-caused fire ignitions and fire occurrence patterns (Parisien et al. 2012, Syphard and Keeley, 2015, Mann et al. 2016, Syphard et al. 2018, Syphard et al. 2019). We tested distance to several road classes: primary and secondary (highways, freeways, US routes, state routes); primary, secondary, and major (county routes, forest routes, National Scenic Byways); primary, secondary, major, and minor (residential, unclassified); and all roads (including very small roads such as service roads). For each subregion, we used only the best performing versions of road variables (see 'Variable Selection' under 'Modeling Process' below).

While spatial data for lightning strikes are available, they are at too coarse in resolution to be useful in this application. Lightning-ignited fires have been shown to be correlated with terrain complexity (McRae 1992, Vazquez and Moreno 1998, Kilinc and Beringer 2007) and fuel moisture (Podur et al. 2003; Wotton and Martell 2005). Terrain and fuel moisture variables are described below.

Climate and weather are regarded as controlling factors of fire occurrence, size, and severity (Westerling et al. 2006, Littell et al. 2009, Dennison et al. 2014, Harvey et al. 2016). Such factors influence whether an ignition may develop into a large, high-severity fire via effects on fuel moisture, structure, and abundance, as well as their real-time effects on fire behavior (e.g., due to wind). Several studies have demonstrated correlations between fire occurrence and size and summer temperatures and precipitation in the Pacific Northwest (McKenzie et al. 2004, Littell et al. 2010, Davis et al. 2017). We therefore tested several temperature, moisture, and humidity-related variables as well as actual evapotranspiration, which is regarded as a proxy for the amount of fuels, and climatic water deficit, considered a proxy for fuel condition and moisture content (Table 3).

Following Parisien et al. (2012), Davis et al. (2017), Tracy et al. (2018), and Syphard et al. (2018 and 2019), we used long-term climate normals as references of relative conditions likely at each location. Climate normals represent the typical state based on averaged conditions from an area over decades of time (Davis et al. 2017). The use of long-term climate normals thus allows for projecting these models forward under different climate Coupled Model Intercomparison Project phase 5 (CMIP5) models, as downscaled projections are available as 30-year averages (<https://adaptwest.databasin.org/pages/adaptwest-climatena>). Although finer-scale, real-time weather conditions during a fire would better predict actual fire effects, such data are non-existent across the entire area of interest or extremely difficult to assemble, and the scope of this project was to predict broad, general patterns to inform management decisions (e.g., forest restoration treatments), not to predict behavior of individual fires.

Vegetation is generally the fuel required for a fire to ignite and spread. Incorporating vegetation structure into a long-term fire model is difficult due to its highly dynamic nature relative to available vegetation data sets. We tested several such predictors, including live tree biomass, live tree density, canopy cover, stand density index, snag biomass, down wood biomass, canopy bulk

density, and canopy base height. The response plots from models using these variables were counterintuitive and suggested there were frequent temporal mismatches between time of fire and time of vegetation mapping (e.g., post-fire vegetation structure variables often did not reflect vegetation structure at the time of the fire). This would thwart our intent of mapping how pre-fire conditions affect severe fire risk. Therefore, similar to Bar Massada et al. (2012) and Syphard et al. (2018), we needed to limit our vegetation predictors to coarse vegetation type, which is less dynamic and has been shown to be an important predictor of fire severity in the Klamath Mountains (Estes et al. 2017) and across the western U.S. (Liu and Wimberly 2015).

Terrain is known to have a direct influence on fire behavior and to indirectly influence fuel flammability (Syphard et al. 2019). Estes et al. (2017) found topographic complexity most strongly influenced fire severity in the Klamath Mountains. Southern aspect and elevation were found by Alexander et al. (2006) to be correlated with fire severity for two fires in the Klamath Siskiyou region. We therefore tested several terrain variables relating to topographic complexity, aspect, and exposure, including elevation, slope, solar insolation index, southwestness index, topographic wetness index (a proxy for soil moisture), and topographic heterogeneity (Table 3).

## Modeling Process

We developed statistical models of large, high-severity fire risk using MaxEnt (distribution model for presence-only data; Version 3.3.3k, Phillips et al. 2006) across the entire Klamath area and separately by the four subregions. MaxEnt compares occurrence points with a sample of background points to create a prediction of relative risk. Similar methods have been successfully used in a range of wildfire analyses (Bar-Massada et al. 2012, Parisien et al. 2016, Davis et al. 2017, Syphard et al. 2018, Tracy et al. 2018, Syphard et al. 2019).

Our modeling process consisted of 3 main steps: (1) variable selection (testing predictors independently and evaluating predictor collinearity), (2) multivariate model creation and variable pruning to create a parsimonious predictive model, and (3) model tuning to control for overfitting. Our models were run in MaxEnt using the default parameters, including model clamping, with the following exceptions: linear, quadratic, and product feature types only, and 10-fold cross-validated replication. Linear, quadratic, and product feature types are preferred to ensure smoother response curves (Santos et al. 2017) and because responses to ecological gradients are frequently nonlinear and interactions among predictors are common. Clamping restricts MaxEnt model extrapolations according to the limits of predictor variables used to train the model and is important when models are projected onto future conditions or new geographic areas, although this should have minimal impacts in this particular application.

Before using all candidate predictors in a full multivariate model, we conducted a correlation analysis on the predictors using ENMTools (version 1.3, Warren et al. 2010). To create more parsimonious and interpretable results (Merow et al. 2013), we excluded correlated variables ( $|r| > 0.7$ , see Appendix 1 for correlation matrix) by selecting the one with the highest univariate 10-fold cross-validated mean AUC (Area Under the Receiver Operating Characteristic (ROC) curve, a threshold-independent assessment of model discriminatory ability, Fielding and Bell 1997). Remaining predictors were carried forward to a full model.

We pruned the resulting full (multivariate) models in an iterative, stepwise process to increase model parsimony by removing the variable contributing the least information to model fit (highest mean training gain without the variable) to decrease model complexity and increase performance (Warren et al. 2014, Yiwen et al. 2016). The model was run again with the remaining predictors. This was repeated until only one variable remained. From the resulting model set, we selected the model with the fewest predictors having a mean training gain not significantly different than the full model. Significance was defined as lack of overlap of 95% confidence intervals for training gain means (calculated in R version 3.5.1; R Core Team 2013). While selected models may include predictors that seemingly have low importance, dropping these predictors results in a statistically significant decrease in model performance.

To prevent model overfitting and reduce complexity, we next tuned our selected model by varying MaxEnt's regularization multiplier parameter to constrain model complexity (Anderson and Gonzalez 2011, Merow et al. 2013, Radosavljevic and Anderson 2014, Warren et al. 2014). We varied the parameter from 0 to 5 in increments of 0.5 (default = 1), and used ENMTools 'Model Selection' function to calculate AICc (Akaike information criterion corrected for small sample sizes) for each (Warren and Seifert 2011)<sup>3</sup>. For this analysis, MaxEnt was run with the variables from the selected pruned model, but using the 'raw' output and no replicates (required for model selection with ENMTools). We selected as the best model the one with the lowest AICc. AICc provides a quantitative measure balancing model complexity and goodness-of-fit without requiring a large independent evaluation dataset (Galante et al. 2018). The model with the lowest AICc is regarded as the best model tested, but all models with AICc values within 2 AICc units (dAICc) are considered to be supported and may be averaged using AICc weights. Rather than averaging models that vary only in terms of their regularization parameter if dAICc < 2, we instead opted for parsimony by simply selecting the regularization parameter with the minimum AICc.

We then ran MaxEnt Klamath-wide and for each subregion with the logistic output option and 10-fold cross validation with the selected regularization parameters to get final output grids using our multivariate tuned models. Subregional model outputs were mosaicked together to create a continuous region-wide grid.

## Model Evaluation

We evaluated model performance using both threshold-dependent and threshold-independent methods. For threshold-dependent, we used the equal training sensitivity and specificity (ESS) metric, which has been shown to be robust at balancing overestimates vs underestimates in MaxEnt predictions (Cao et al. 2013). We used the ESS thresholds provided by MaxEnt (Table 4) to reclassify our continuous model outputs into binary 'high risk' (>ESS) and 'low risk' (< ESS) grids. These were intersected with the reserved high-severity and low-severity test points to calculate model sensitivity (True Positive / (True Positive + False Negative)), specificity (True Negative / (False Positive + True Negative)), and accuracy ((True Positive + True Negative) / (Positive + Negative)). We also calculated the percent of high-severity and low-severity pixels overlapping the binary outputs.

---

<sup>3</sup> We did this because Maxent does not provide this information.

While our models were derived using fire data from 1984 to 2010 to match the temporal extent of the climate data, additional data for independent model evaluation are available from 2011 to 2015. We calculated the percent of 2011 to 2015 high-severity and low-severity pixels that were correctly classified by overlaying them with the thresholded model outputs.

For threshold-independent evaluation metrics, we calculated the point-biserial correlation (Pearson’s product-moment correlation) between the continuous model outputs and the high- and low-severity test points (Elith et al. 2006). We also tested for differences in the mean fire risk values between low- and high-severity test point groups using a Welch two sample t-test.

Mean 10% test omission rates and difference between testing and training AUC values ( $AUC_{diff}$ ) were examined to evaluate potential model overfitting. We also report test AUC values, but this model evaluation statistic has been shown to be sensitive to sample size (Lobo et al. 2007), making comparisons between models using different occurrence data difficult.

**Table 4.** Equal training sensitivity and specificity (ESS) thresholds used to subdivide the MaxEnt model continuous value outputs into high risk vs low risk areas for large, severe wildfire for purposes of model testing.

Region-wide	Subregion 1a	Subregion 1b	Subregion 2	Subregion 3
0.414	0.395	0.393	0.315	0.284

## Results

These results represent outputs from statistical models based on available landscape-scale GIS variables that cannot account for real-time fire conditions. They describe broad geographic patterns in landscape fire risk across the entire Klamath region and broken down by subregions. The region-wide model balances statistical influences on fire severity across very broad ecological and climatic gradients, thus revealing broad patterns which may be interesting but not necessarily very useful for on-ground management decisions. Subregional models are more discriminating of conditions affecting fire risk over a narrower range of environmental conditions (e.g., within a hotter-drier landscape or within a cooler-moister landscape), and thus provide more pertinent information for management decisions. All model outputs should be considered hypotheses to be refined with additional information.

### High-severity Fire Risk Models

Topographic heterogeneity (“ruggedness”), annual heat moisture index, and vegetation class were the predominant predictive variables in the Klamath-wide model. Projected fire risk varies greatly

across the Klamath region, but is concentrated in the more westerly and heavily forested subregions 1a and 1b, with more scattered areas of high risk in the more arid shrub-dominated east subregions 2 and 3 (Figure 3 and Figure 4, left). Large areas of severe fire risk are predicted within the interior Northern California Coast Ranges and the Klamath Mountains, with smaller concentrations in the West Cascades, Sierra Nevada Foothills, and Sierra Nevada and the Warner Mountains.

The results suggest that, very broadly across this diverse region, fire risk is generally associated with rugged terrain and relatively warm-dry conditions--but the patterns are complicated by complex interactions amongst variables across this very broad eco-climatic gradient. For example, the predominant fuel is conifers in some high-fire areas (especially in moister coastal subregions) and shrubs in other areas (especially in drier inland areas). Given that forest and shrubland vegetation communities reflect the environmental conditions supporting them, and that these same environmental conditions affect fire severity via other means--e.g, real-time weather and fuel conditions--these broad patterns may obscure finer-scale insights.

Subregional models reveal finer-scale variation in how fire risks vary with landscape variables. In subregion 1, areas of high risk are concentrated in the Eastern Franciscan ecoregional subsection (Figure 3 and Figure 4). The Rattlesnake Creek, Trinity Mountain-Hayfork, North Trinity Mountain, Eastern Klamath Mountains, Upper Salmon Mountains, Siskiyou Serpentine, and Siskiyou Mountains ecoregional subsections within the Klamath Mountains contain the largest concentration of high risk areas within subregion 1b (Figure 3 and Figure 4). These areas support dense forests in somewhat warmer, drier conditions than more coastal forests.

Within subregion 2, high fire risk is concentrated in the south in the Sierra Nevada (Granitic and Metamorphic Foothills, Diamond Mountains-Crystal Peak, Fredonyer Butte-Grizzly Peak, and Greenville-Graeagle ecoregional subsections), portions of the Shingletown-Paradise ecoregional subsection within the southern Cascades, and in the Western Cascades Highland Forest ecoregional subsection (Figure 3 and Figure 4).

Predicted high fire risk in subregion 3 is concentrated in dry shrub and conifer vegetation in mid-elevation areas of the Modoc Plateau (Fremont Pine-Fir Forest, Warner Mountains, Mountains and Valleys, Likely Mountain, Big Valley Mountains, and Eagle Lake-Observation Peak ecoregional subsections) and portions of the Northwestern Nevada Ranges and the Eastern Cascades' Pumice Plateau Forest (Figure 3 and Figure 4).

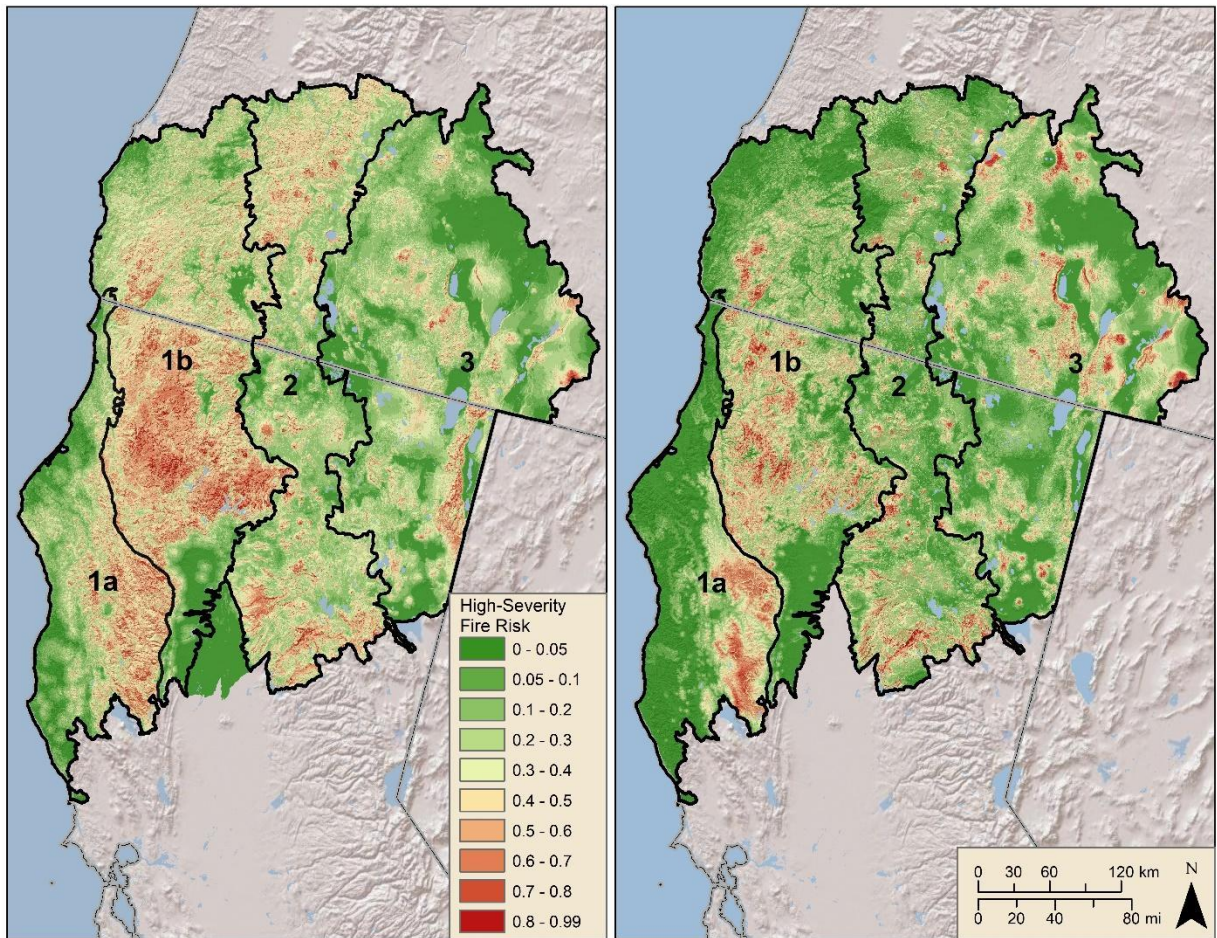


**Figure 3.** Modeled large high-severity fire risk using a region-wide model (left) and four subregional models (right).

Variables selected in final models differed among subregions, as expected. Nevertheless, each model included at least one each of a climate, topographic, development, and vegetation variable. Differences in variable importance by subregion suggest that fire-environment relationships are complex and varied across the broad and ecologically diverse Klamath area (see Appendix 2 for variable response plots).

Vegetation type was the only predictor common to all models, with its importance ranging from 3.4 in subregion 1a to 27.1 in subregion 2 (Table 5). The model for subregion 1a is largely driven by distance to public lands, while in subregion 1b, distance to public lands and elevation are nearly equal in greatest importance. In both subregions, large, high-severity fire risk is concentrated closer to public lands than private lands, which probably reflects differences in vegetation and fire-fighting actions between public and private lands. Although fire ignitions are concentrated near development and roads, fires on wild public lands are more likely to become large and severe due to rugged terrain, vegetation characteristics, and fire-fighting priorities and access.

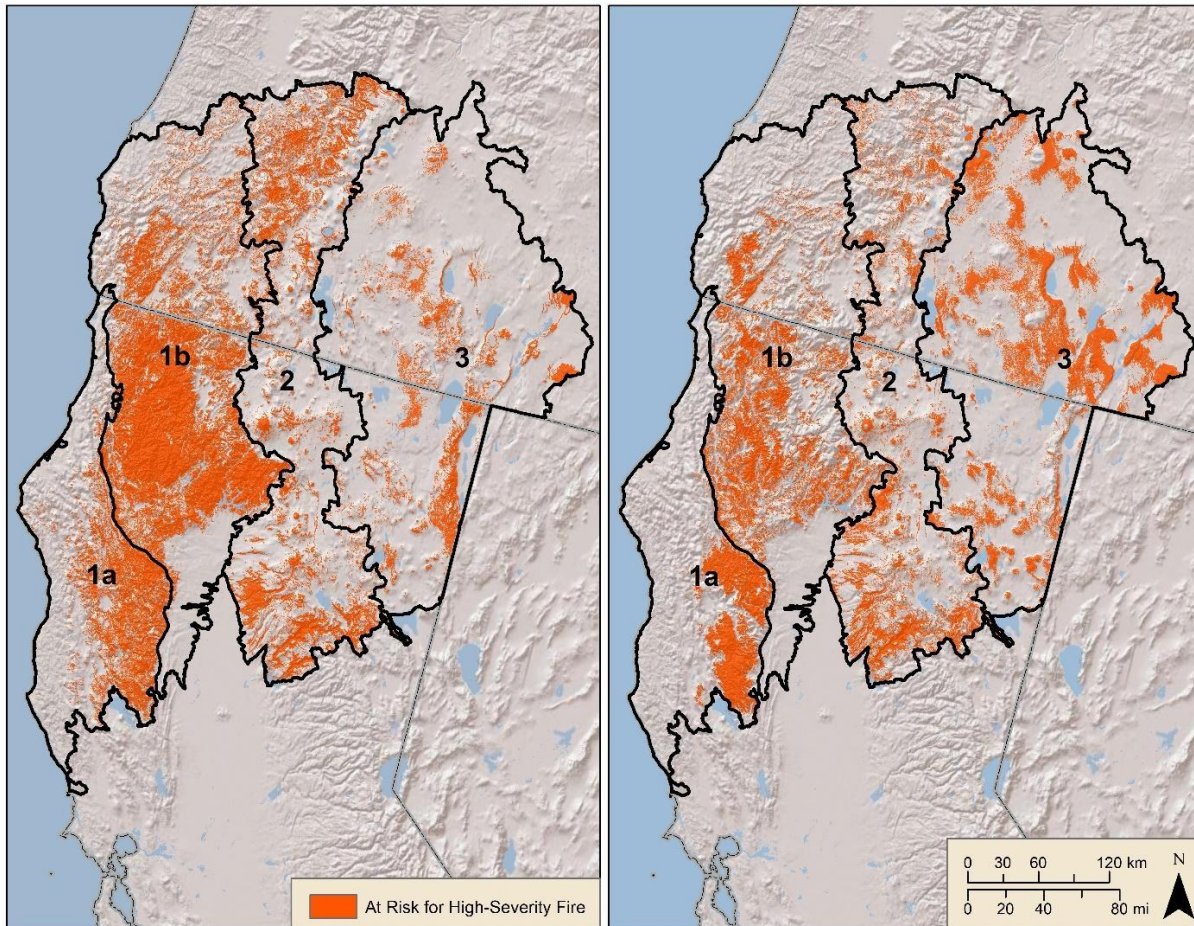


**Figure 4.** Modeled large high-severity fire risk using a region-wide model (left) and subregional models (right), classified as ‘at risk’ using equal sensitivity and specificity thresholds.

Mapped outputs of the Klamath-wide model and the subregional model mosaics differed (Figure 5) although there was just a 5% difference in the total area predicted at risk of severe fire (25% by Klamath-wide and 20% by the subregional models, Figure 5). The thresholded models agree across 80% of the overall region, with the Klamath-wide model predicting about 12% of the region at risk and the combined subregional models predicting about 8% of the overall region (Figure 5). Comparing the orange and yellow areas on Figure 5, it appears the subregional models are more discriminating of fire risk in general, and that the region-wide model may especially under-predict the extent of risk in subregion 3.

**Table 5.** Predictor importance determined by MaxEnt for regional and subregional fire risk models.

<b>Predictor</b>	<b>Region- wide</b>	<b>Subregion 1a</b>	<b>Subregion 1b</b>	<b>Subregion 2</b>	<b>Subregion 3</b>
Vegetation Type	21.9	3.4	13.5	27.1	9.0
Distance to Public Lands	9.5	49.1	23.0	2.6	
Distance to Development	4.4		7.6	2.8	20.7
Distance to Primary/Secondary Roads		10.4		16.5	11.2
Distance to Major and Minor Roads			5.9		
Mean Annual Precipitation		3.1	3.6	15.3	
Difference between MCMT and MWMT (measure of continentality)	9.5			7.6	10.7
Mean Annual Relative Humidity			3.6		13.2
Annual Heat Moisture Index	23				7.5
Summer Heat Moisture Index		11.0			
Mean Temp Warmest Month (MWMT)		4.2			
Wind		1.9			
Annual Maximum Vapor Pressure Deficit			6.7		
Precipitation as Snow					18.0
Mean Temp Coldest Month (MCMT)				6.8	
Topographic Heterogeneity	31.6		11.1	14.1	5.4
Southwestness			2.6	1.2	1.4
Elevation		17	22.5		2
Insolation Index				6	0.9

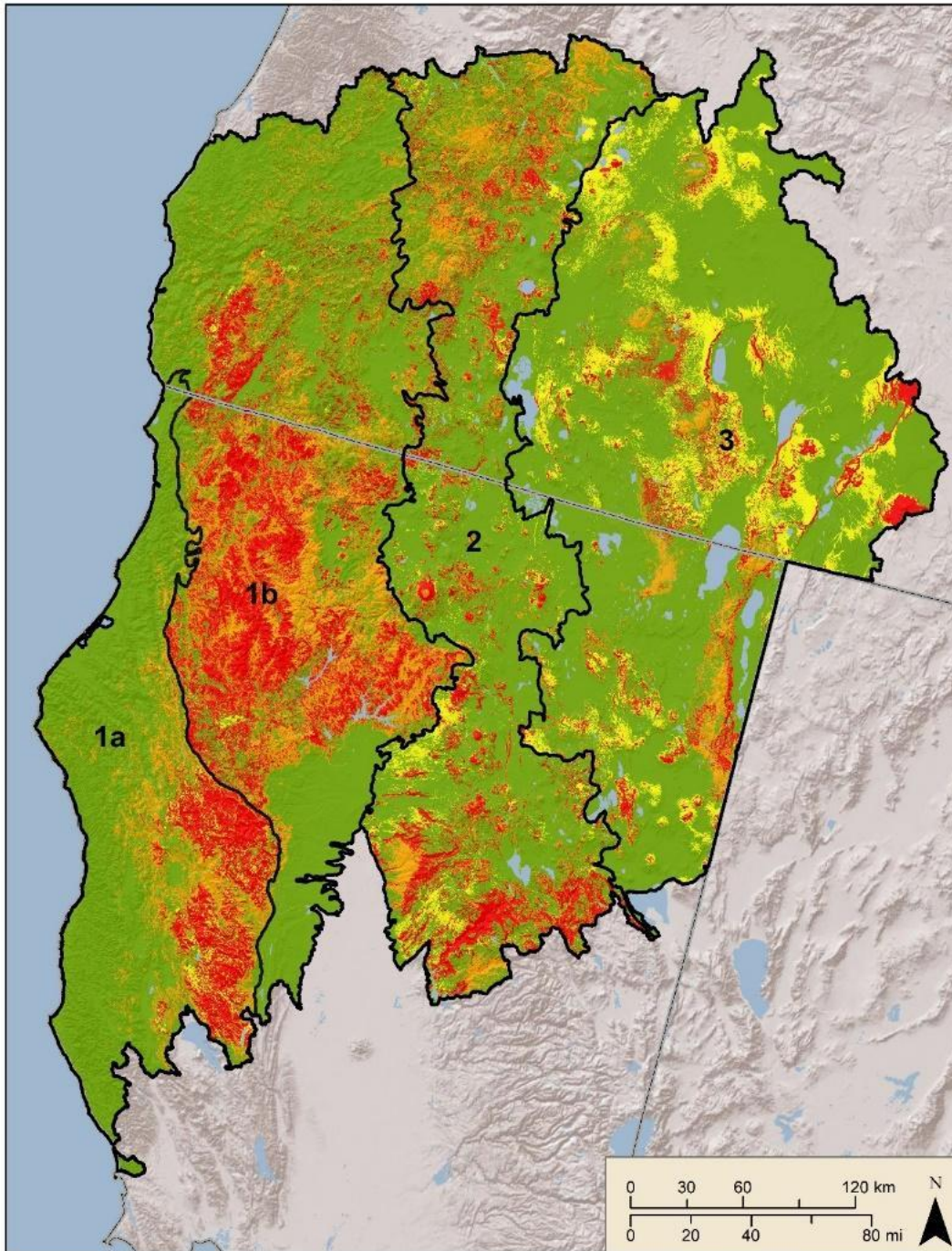


**Figure 5.** Agreement between region-wide and subregional fire risk models. Red indicates high risk and green low risk predicted by both regional and subregional models; orange indicates high risk predicted by the region-wide model only; and yellow indicates high risk by subregional models only.

Model average test AUC values, a measure of model discrimination, were good across all selected models (Araujo et al. 2005), ranging from 0.8 for the region-wide model to 0.87 in subregions 1a and 3 (Table 6). We repeat that fire modeling is inherently uncertain given the stochastic nature of fire and how it is affected by factors not yet mapped and available for statistical analyses, and that these results must be interpreted with due caution.

Mean 10% omission rates ranged from 0.10 (Klamath-wide model) to 0.16 in subregion 1b and AUC<sub>diff</sub> values ranged from 0.03 (Klamath-wide model) to 0.07 in subregion 1a, suggesting no model suffered from overfitting. The combined subregional models outperformed the Klamath-wide model by most evaluation metrics, as expected. The Klamath-wide model had slightly lower overall accuracy and lower correct classification rates of low-severity fire, but higher classification rates for high-severity fire than the combined subregional models (Table 6).

**Table 6.** Evaluation metrics for region-wide and subregional models.

Metric	Region-wide	Subregional combined	Region 1a	Region 1b	Region 2	Region 3
Mean Test AUC	0.8	-	0.87	0.81	0.83	0.87
Mean AUC <sub>diff</sub>	0.03	-	0.07	0.06	0.05	0.04
Mean 10% Test Omission	0.1	-	0.12	0.16	0.14	0.12
Sensitivity	0.69	0.65	0.67	0.6	0.72	0.67
Specificity	0.5	0.60	0.67	0.43	0.69	0.68
Accuracy	0.59	0.63	0.67	0.51	0.71	0.68
Pearson's product-moment correlation (p-value)	0.229 (0.001)	0.306 (0.00001)	0.172 (0.420)	0.093 (0.398)	0.526 (0.00002)	0.469 (0.004)
t (p-value)	3.329 (0.001)	4.543 (0.00001)	0.821 (0.422)	0.850 (0.398)	4.624 (0.00003)	3.094 (0.004)
Classification High Severity, 1984-2010	69.2	67.6	76.3	58.3	74.6	80.3
Classification Low Severity, 1984-2010	44.5	55.8	43.8	50.1	62.2	65.6
Classification High Severity, 2011-2015	56	36.6	26.2	43.2	23.5	36.6
Classification Low Severity, 2011-2015	51	70.4	83.6	62.8	72.4	75.5

Model sensitivity (proportion of high-severity points correctly classified) ranged from 0.6 (subregion 1b) to 0.72 (subregion 2), while specificity (proportion of low-severity points correctly classified) was highest in subregion 1a (0.7) and lowest in subregion 1b (0.43; Table 6). Overall accuracy was highest in subregion 2 (0.71) and lowest in subregion 1b (0.51). Low evaluation metrics are to be expected given that these models do not account for real-time fire conditions and fire-fighting effects.

All models performed better at capturing high-severity pixels than at correctly classifying low-severity pixels (Figure 6, Table 6), which is not surprising given that the statistical models were trained to predict high-, not low-, severity fire risk using high-fire sample points. The percent of high-severity pixels correctly classified ranged from a low of 58.3 in subregion 1b to a high of 80.3 in subregion 3. The percent of low-severity pixels correctly classified was highest in subregion 3 and lowest in subregion 1a.

All models performed poorly at correctly classifying high-severity fires that occurred *after* the time period of the occurrence data used to train them (Figure 7, Table 6). Correct classification of high-severity fires from 2011 to 2015 was highest in the region-wide model (56.0) and lowest in subregion 1a (26.2). Low-severity fire classification rates from 2011 to 2015 were much higher, ranging from a low of 51.0 for the Klamath-wide model to 83.6 in subregion 1a. These results could reflect effects of the 2011-16 drought on fire conditions and again re-emphasize the importance of matching variables in time as well as space to understand changing fire patterns.

Threshold-independent evaluation metrics showed significant differences in modeled risk values between high and low severity test points in both the region-wide and combined sub-regional models (correlations were 0.306 for combined sub-regional models and 0.229 for region-wide model; t-tests for differences in mean risk values between groups were significant; Table 6).

Our results suggest that fire patterns and drivers of large, high-severity fire in the Klamath region vary substantially across this geographically diverse area. There was considerable agreement between the region-wide and subregional models, and neither output was superior across all evaluation metrics used. The region-wide model is better at capturing high-severity fires during both time periods tested, while the subregional models are better at classifying low-severity fires during both time periods. Subregional models likely better reflect finer-scale fire-environment relationships compared to the Klamath-wide model, and therefore may better inform management decisions. We recommend using the continuous rather than thresholded model outputs to better demonstrate the full range of risk across the landscape, and of course considering other information bearing on fire risks when applying these results.

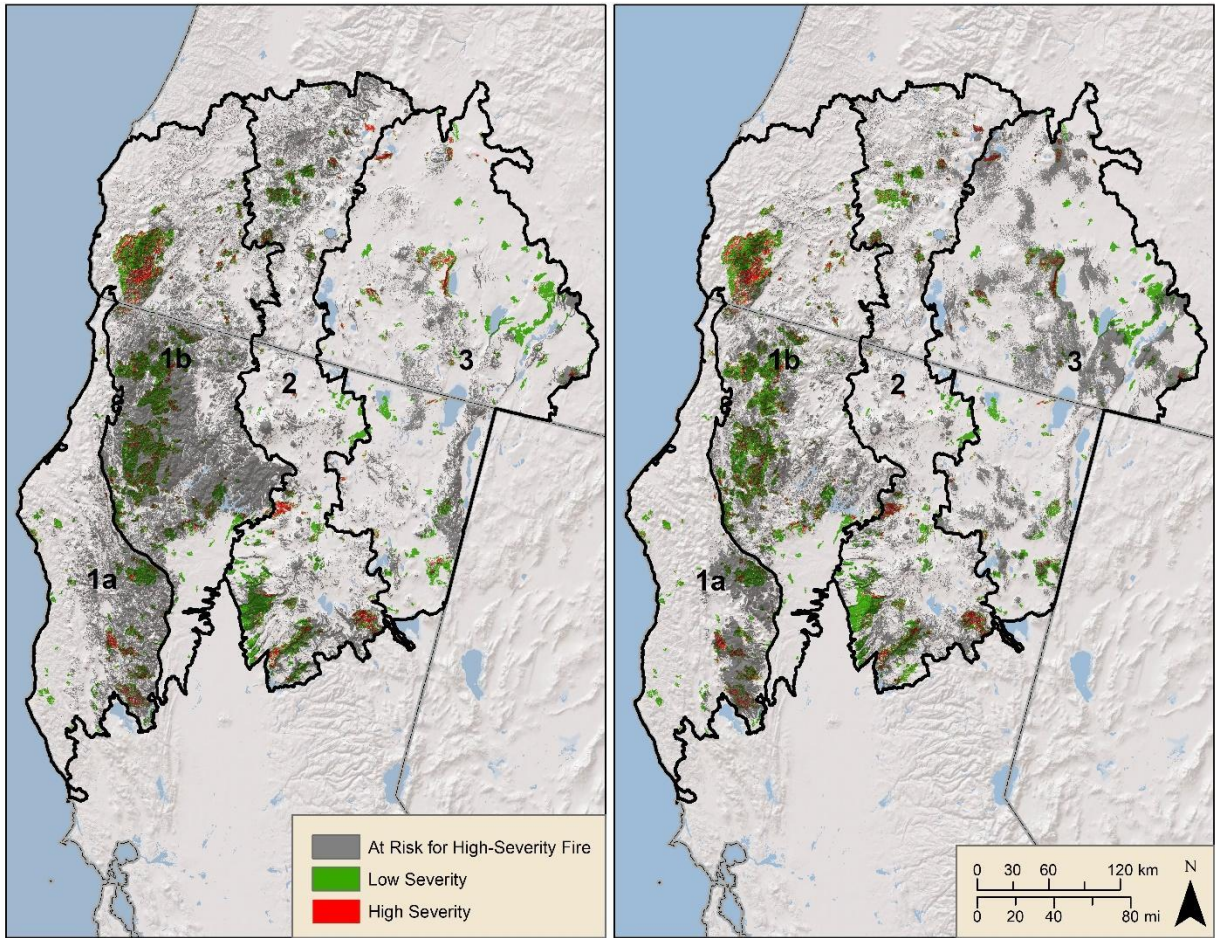


**Figure 6.** Overlap between modeled large, high-severity fire risk (gray) using a region-wide model (left) and subregional models (right), classified as ‘at risk’ using the equal sensitivity and specificity threshold, and actual mapped low (green) and high (red) burn severity areas, 1984-2010 (MTBS, USDA Forest Service/U.S. Geological Survey, <https://mtbs.gov/>).

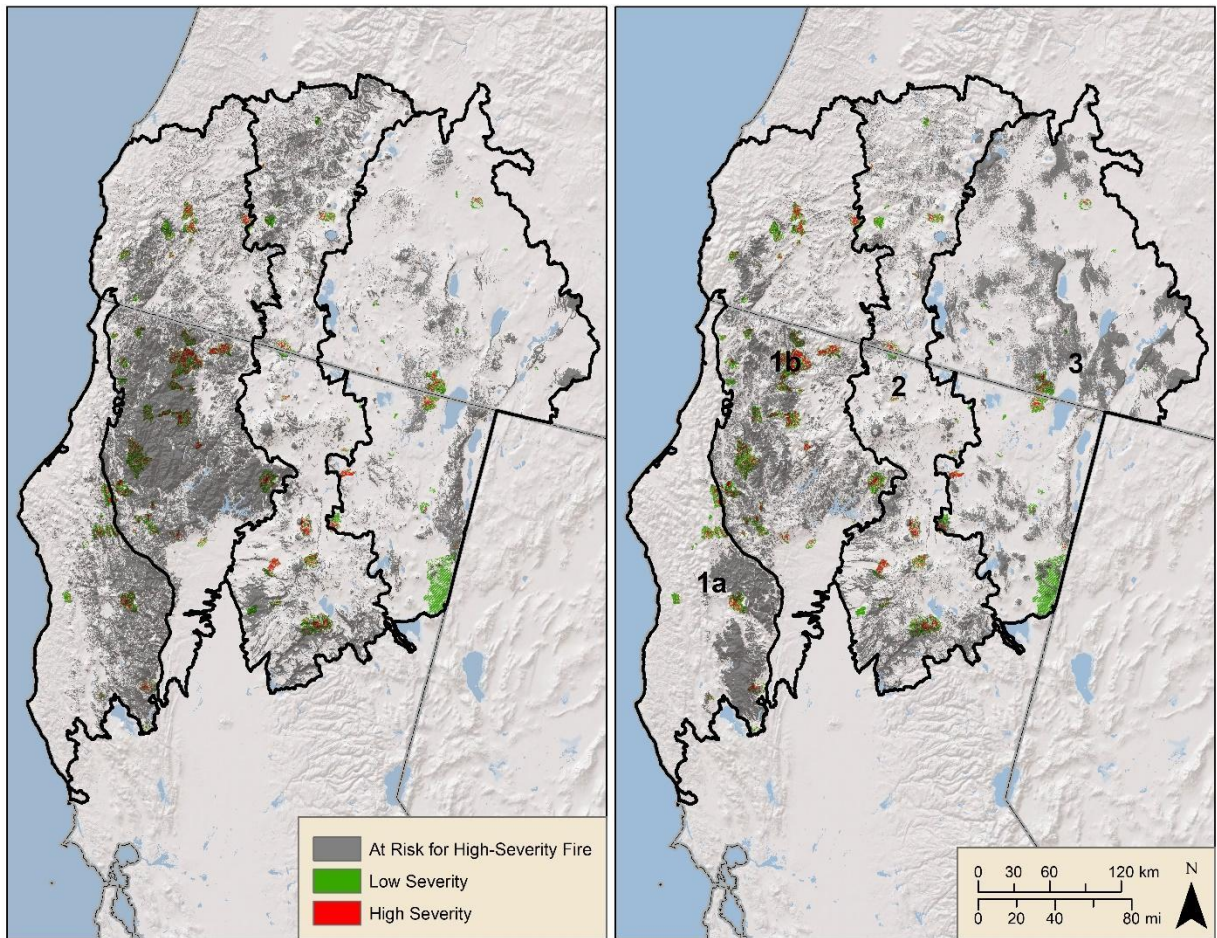


**Figure 7.** Overlap between modeled large, high-severity fire risk (grey) using a region-wide model (left) and subregional models (right), classified as ‘at risk’ using equal sensitivity and specificity thresholds, and actual mapped low (green) and high (red) burn severity areas, 2011-2015 (MTBS, USDA Forest Service/U.S. Geological Survey, <https://mtbs.gov/>).

### Potential Impacts of Severe Fire on Fisher and Marten Core and Linkage Habitats

We overlaid results of the subregional fire risk model with fisher and marten cores and corridors delineated by Spencer et al. (2019; USFWS Cooperative Agreement F17AC00856) to evaluate where high-priority fisher and marten habitat areas may be at greatest risk of loss to fires. Results are shown in Figures 8 and 9, and summary statistics are presented in Table 7. The results suggest that important core and linkage habitats for fisher are at risk of at least temporary loss due to severe fires, especially in the Klamath and Coast Ranges and the northern Sierra Nevada-Southern Cascade regions of northern California. Marten core habitat areas appear to have lesser risk of loss, but some tenuous connectivity areas appear to be at high risk, especially between the Lassen and Shasta regions and the Warner Mountains and Klamath region. These results should be considered when prioritizing management interventions intended to reduce fire risks in forested areas.

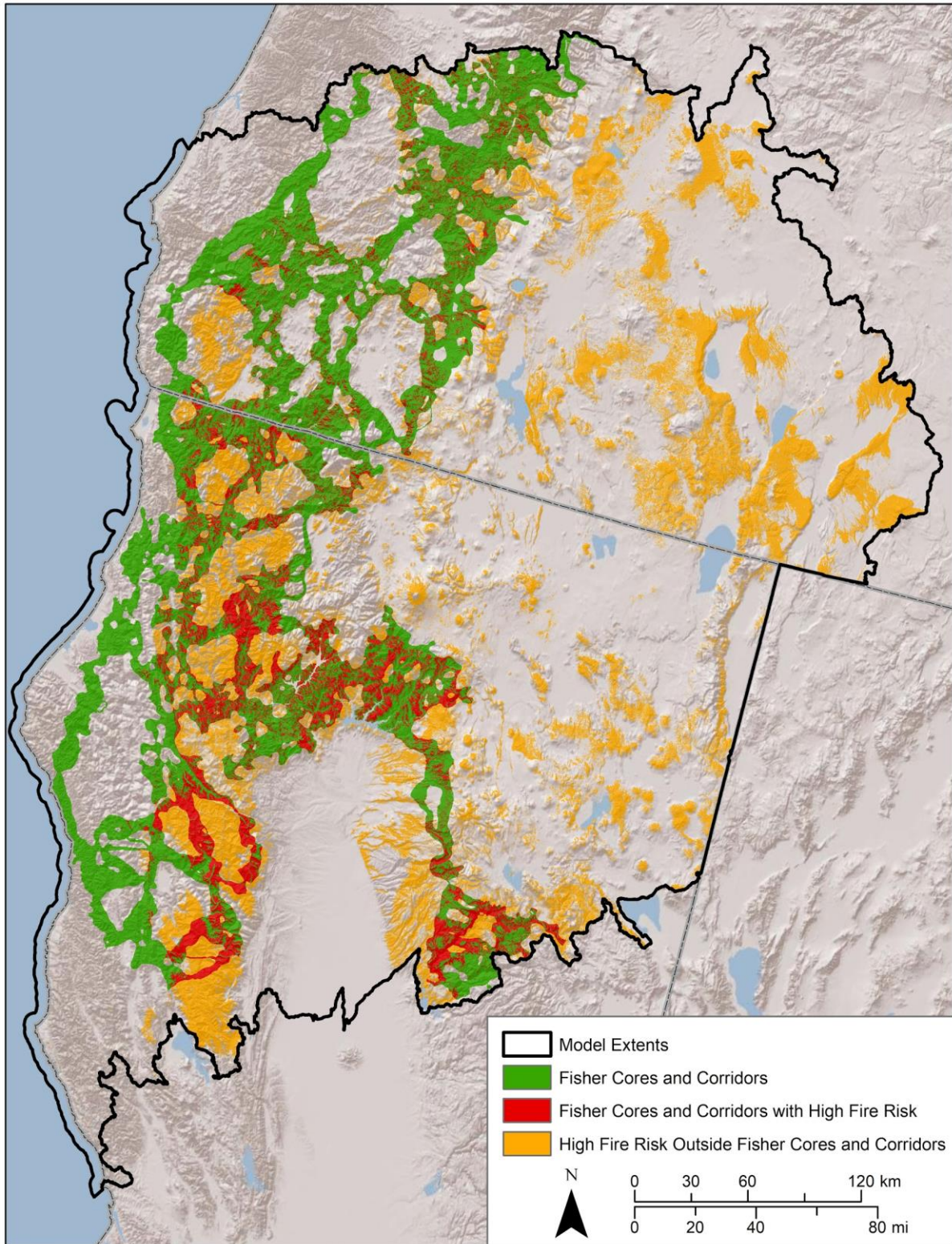


**Figure 8.** High-severity fire risk overlaid with fisher core and linkage habitats.

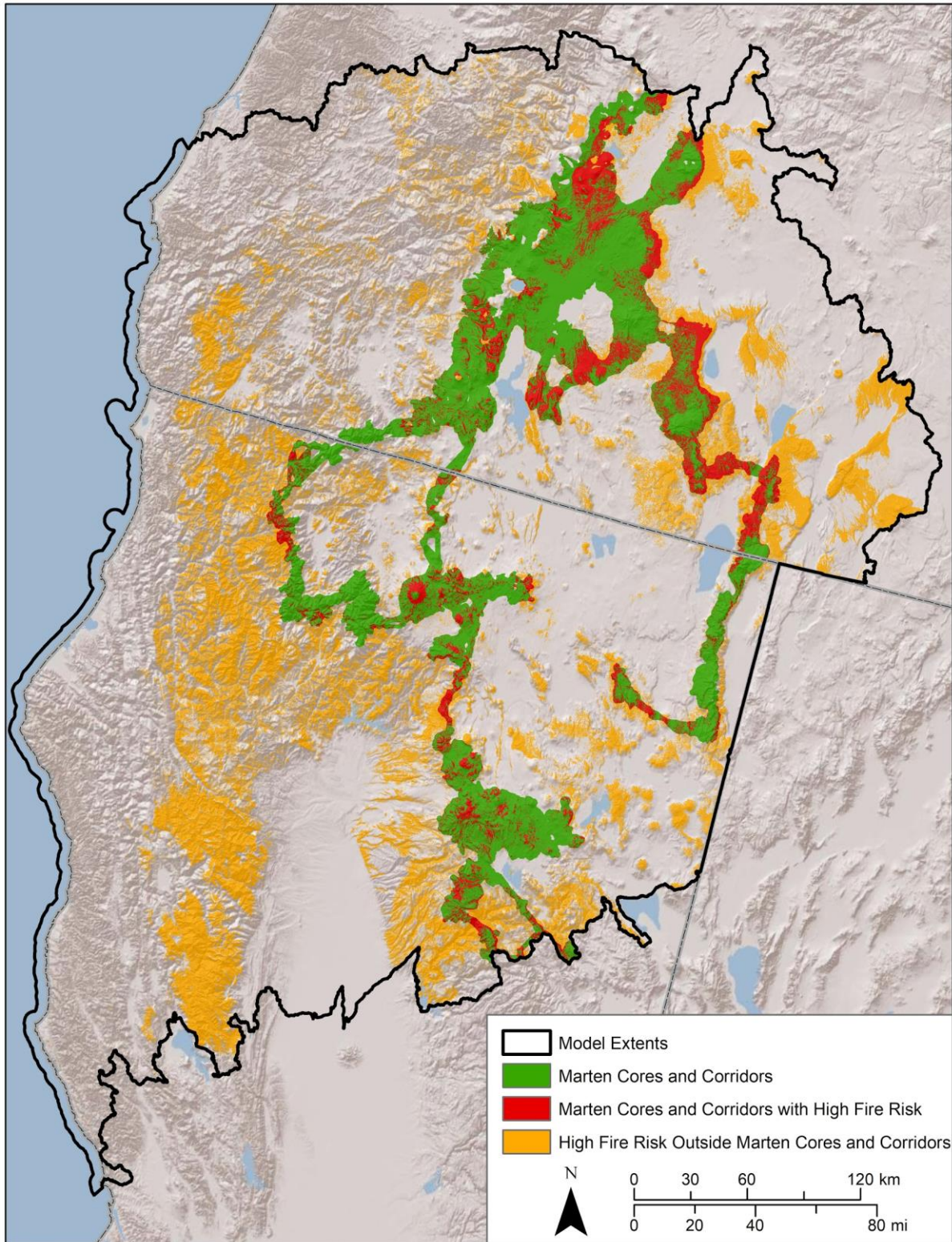


**Figure 9.** High-severity fire risk overlaid with marten cores and linkages.

**Table 7.** Correspondence between high fire risk areas and fisher and marten core and linkage habitats in the Klamath study region.

<b>Habitat Component</b>	<b>Acres at Risk</b>	<b>% at Risk</b>
Fisher Cores	1,340,506	24%
Fisher Linkages	1,031,907	24%
Marten Cores	484,272	21%
Marten Linkages	1,042,693	30%

## Data Products

Results of this project are available as maps and data that can be viewed and downloaded from Data Basin. We recommend the user go directly to the Data Basin gallery linked below, or use the index below to access individual products.

### [Klamath Large, High-severity Fire Risk Modeling Gallery](#)

#### Fire Risk Model Outputs

1. [Areas at Risk of Large High-severity Fire, Mosaic of Subregional Models, Greater Klamath Region, OR and CA](#)
2. [Areas at Risk of Large High-severity Fire, Region-wide Model, Greater Klamath Region, OR and CA](#)
3. [Large High-severity Fire Risk, Region-wide Model, Greater Klamath Region, OR and CA](#)
4. [Large High-severity Fire Risk, Mosaic of Subregional Models, Greater Klamath Region, OR and CA](#)

#### Input Data for Fire Risk Model

1. [Klamath High-severity Fire Points, Region-wide Model, 1984-2010](#)
2. [Klamath High-severity Fire Points, Subregional Models, 1984-2010](#)
3. [Predictors for Klamath Region-wide Large, High-severity Fire Risk Model](#)
4. [Predictors for Klamath Large, High-severity Fire Risk Model \(Subregion 1a\)](#)
5. [Predictors for Klamath Large High-severity Fire Risk Model \(Subregion 1b, Part 1\)](#)
6. [Predictors for Klamath Large High-severity Fire Risk Model \(Subregion 1b, Part 2\)](#)
7. [Predictors for Klamath Large High-severity Fire Risk Model \(Subregion 2, Part 1\)](#)
8. [Predictors for Klamath Large High-severity Fire Risk Model \(Subregion 2, Part 2\)](#)
9. [Predictors for Klamath Large High-severity Fire Risk Model \(Subregion 3, Part 2\)](#)
10. [Predictors for Klamath Large High-severity Fire Risk Model \(Subregion 3, Part 1\)](#)
11. [Subregions for Klamath Large, High-severity Fire Risk Modeling](#)

#### Overlay Analysis for Fisher and Martin

1. [Fisher Cores and Linkages with High Fire Risk, Klamath](#)
2. [Marten Cores and Linkages with High Fire Risk, Klamath](#)

## Literature Cited

- Alexander, J.D., N.E. Seavy, C.J. Ralph, and B. Hogoboom. 2006. Vegetation and topographical correlates of fire severity from two fires in the Klamath-Siskiyou region of Oregon and California. *International Journal of Wildland Fire* 15: 237-245.
- Anderson, R.P. and I. Gonzalez, Jr. 2011. Species-specific tuning increases robustness to sampling bias in models of species distributions: an implementation with MaxEnt. *Ecological Modelling* 222: 2796-2811.
- Araujo, M. B., R.G. Pearson, W. Thuiller, and M. Erhard. 2005. Validation of species-climate impact models under climate change. *Global Change Biology* 11: 1504-1513.
- Bar-Massada, A., A.D. Syphard, S.I. Stewart, and V.C. Radeloff. 2012. Wildfire ignition-distribution modelling: a comparative study in the Huron–Manistee National Forest, Michigan, USA. *International Journal of Wildland Fire* 22: 174–183.
- Boria, R.A., L.E. Olson, S.M. Goodman, and R.P. Anderson. 2014. Spatial filtering to reduce sampling bias can improve the performance of ecological niche models. *Ecological Modelling* 275: 73–77.
- Cao, Y., R. E. DeWalt, J.L. Robinson, T. Tweddale, L. Hinz, and M. Pessino. 2013. Using MaxEnt to model the historic distributions of stonefly species in Illinois streams: The effects of regularization and threshold selections. *Ecological Modelling* 259: 30-39.
- Davis, R., Y. Zhiqiang, A. Yost, C. Belongie, and W. Cohen. 2017. The normal fire environment – Modeling environmental suitability for large forest wildfires using past, present, and future climate normals. *Forest Ecology and Management* 390: 173-186.
- Dennison PE, S.C., Brewer, J.D. Arnold, and M.A. Moritz. 2014. Large wildfire trends in the western United States, 1984–2011. *Geophysical Research Letters* 41:2928–2933.
- Eidenshink, J.C., B. Schwind, K. Brewer, Z.L. Zhu, B. Quayle, and S.M. Howard. 2007. A project for monitoring trends in burn severity. *Fire Ecology* 3: 3–21.
- Elith J., C.H. Graham, R.P. Anderson, *et al.* 2006. Novel methods improve prediction of species' distributions from occurrence data. *Ecography* 29:129–151.
- Estes, B.L., E.E. Knapp, C.N. Skinner, J.D. Miller, and H.K. Preisler. 2017. Factors influencing fire severity under moderate burning conditions in the Klamath Mountains, northern California, USA. *Ecosphere* 85(5):e01794.10.1002/ecs2.1794
- Fielding, A.H. and J.F. Bell. 1997. A review of methods for the assessment of prediction errors in conservation presence/absence models. *Environmental Conservation* 24: 38–49.

- Franklin, J., 2003. Clustering versus regression trees for determining Ecological Land Units in the southern California Mountains and foothills. *Forest Science* 49: 354–368.
- Galante, P.J., B. Alade, R. Muscarella, S.A. Jansa, S.M. Goodman, and R.P. Anderson. 2018. The challenge of modeling niches and distributions for data-poor species: a comprehensive approach to model complexity. *Ecography* 41: 726-736.
- Gustafson, E.J., S.M. Lietz, and J.L. Wright. 2003. Predicting the spatial distribution of aspen growth potential in the upper Great Lakes region. *Forest Science* 49: 499-508.
- Harvey, B.J., D.C. Donato, and M.G. Turner. 2016. Drivers and trends in landscape patterns of stand-replacing fire in forests of the US Northern Rocky Mountains (1984-2010). *Landscape Ecology* 31: 2367-2383.
- Hernandez, P., C.J. Graham, L.L. Master, and D.L. Albert. 2006. The effect of sample size and species characteristics on performance of different species distribution modeling methods. *Ecography* 29: 773-785.
- Kilinc, M. and J. Beringer. 2007. The spatial and temporal distribution of lightning strikes and their relationship with vegetation type, elevation, and fire scars in the Northern Territory. *Journal of Climate* 20: 1161-1173.
- Littell, J.S., D. McKenzie, D.L. Peterson, and A.L. Westerling. 2009. Climate and wildfire area burned in western U.S. ecoregions, 1916–2003. *Ecological Applications* 19:1003-1021.
- Littell, J. S., E.E. Oneil, D. McKenzie, J.A. Hicke, J. Lutz, R.A. Norheim, and M.M. Elsner. 2010. Forest ecosystems, disturbance, and climatic change in Washington State, USA. *Climatic Change* 102:129-158.
- Liu, Z. and M.C. Wimberly. 2015. Climatic and landscape influences on fire regimes from 1984 to 2010 in the western United States. *PLoS ONE* 10(10): e0140839.  
<https://doi.org/10.1371/journal.pone.0140839>
- Lobo, J. M, A. Jimenez-Valverde, and R. Real. 2007. AUC: a misleading measure of the performance of predictive distribution models. *Global Ecology and Biogeography* 17: 145-151.
- Mann, M.L., E. Batllori, M.A. Moritz, E.K. Waller, P. Berck, A.L. Flint, L.E. Flint, and E. Dolfi. 2016. Incorporating anthropogenic influences into fire probability models: effects of human activity and climate change on fire activity in California. *PLoS One* 11(4): e0153589.
- McKenzie, D., Z. Gedalof, D.L. Peterson, and P. Mote. 2004. Climatic change, wildfire, and conservation. *Conservation Biology* 18: 890–902.

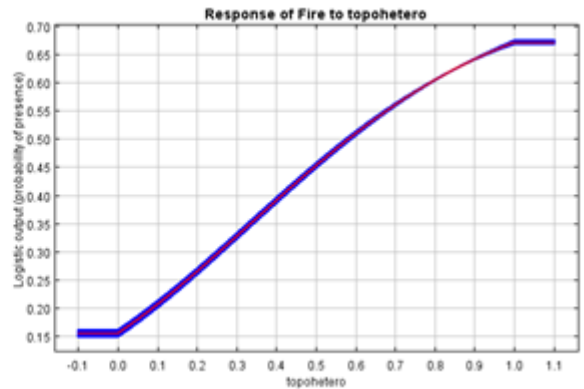
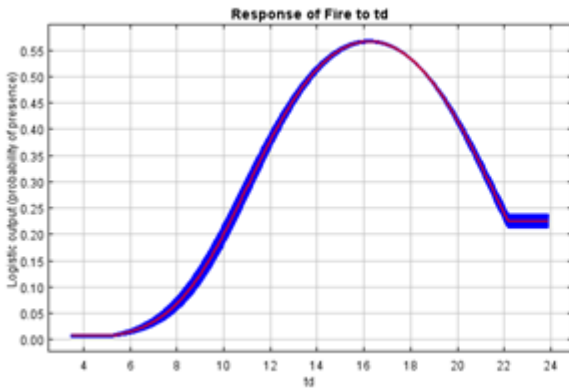
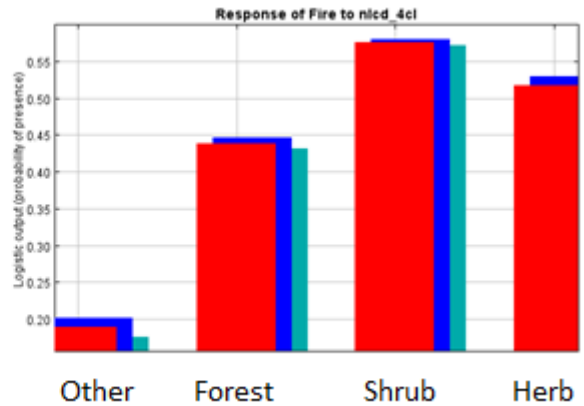
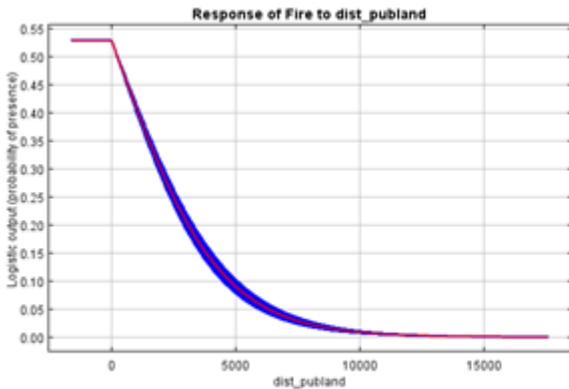
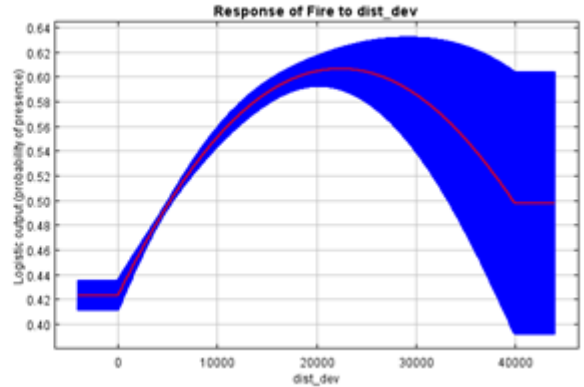
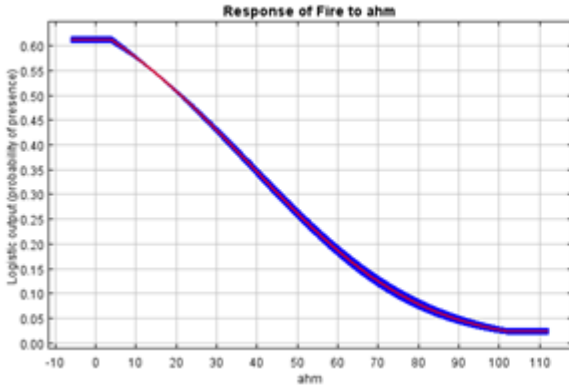
- McRae, R.H.D. 1992. Prediction of areas prone to lightning ignition. *International Journal of Wildland Fire* 2:123-130.
- Merow, C., M.J. Smith, and J.A. Silander, Jr. 2013. A practical guide to MaxEnt for modeling species' distributions: what it does, and why inputs and settings matter. *Ecography* 36: 1058-1069.
- Parisien, M.-A., S. Snetsinger, J.A. Greenberg, C.R. Nelson, T. Schoennagel, S.Z. Dobrowski, and M.A. Moritz. 2012. Spatial variability in wildfire probability across the western United States. *International Journal of Wildland Fire* 21: 313-327.
- Parisien, M.-A., S. Snetsinger, J.A. Greenberg, C.R. Nelson, T. Schoennagel, S.Z. Dobrowski, and M.A. Moritz. 2016. The spatially varying influence of humans on fire probability in North America. *Environmental Research Letters* 11:75005.
- Pearson, R.G., C.J. Raxworthy, M. Nakamura, and A.T. Peterson. 2007. Predicting species distributions from small numbers of occurrence records: a test case using cryptic geckos in Madagascar. *Journal of Biogeography* 34: 102-117.
- Phillips, S. J., R. P. Anderson, and R. E. Schapire. 2006. Maximum entropy modeling of species geographic distributions. *Ecological Modelling* 190:231-259.
- Podur, J., D.L. Martell, F. Csillag. 2003. Spatial patterns of lightning-caused forest fires in Ontario, 1976-1998. *Ecological Modelling* 164: 1-20.
- Radosavljevic, A. and R.P. Anderson. 2014. Making better MaxEnt models of species distributions: complexity, overfitting and evaluation. *Journal of Biogeography* 41: 629-643.
- Santos, M.J., A.B. Smith, J.H. Thorne, and C. Moritz. 2017. The relative influence of change in habitat and climate on elevation range limits in small mammals in Yosemite National Park, California, U.S.A. *Climate Change Responses* 4:7.
- Syphard, A.D. and J.E. Keeley. 2015. Location, timing, and extent of wildfire varies by cause of ignition. *International Journal of Wildland Fire* 24: 37-47.
- Syphard, A.D., T. Sheehan, H. Rustigian-Romsos, and K. Ferschweiler. 2018. Mapping future fire probability under climate change: Does vegetation matter? *PloS one* 13: e0201680.
- Syphard, A.D., H. Rustigian-Romsos, M. Mann, E. conlisk, M.A. Moritz, and D. Ackerly. 2019. The relative influence of climate and housing development on current and projected future fire patterns and structure loss across three California landscapes. *Global Environmental Change* 56: 41-55.
- Tracy, J.L., A. Trabucco, A.M. Lawing, J. T. Giermakowski, M. Tchakerian, G.M. Drus, and R.N. Coulson. 2018. Random subset feature selection for ecological niche models of wildfire activity in Western North America. *Ecological Modelling* 383:52-68.

- Vazquez, A. and J.M. Moreno. 1998. Patterns of lightning-, and people-caused fires in peninsular Spain. *International Journal of Wildland Fire* 8: 103-115.
- Veloz, S.D. 2009. Spatially autocorrelated sampling falsely inflates measures of accuracy for presence-only niche models. *Journal of Biogeography* 36: 2290–2299.
- Warren, D.L., R.E. Glor, and M. Turelli. 2010. ENMTools: a toolbox for comparative studies of environmental niche models. *Ecography* 33: 607-611.
- Warren, D.L., A.N. Wright, S.N. Seifert, and B.H. Shaffer. 2014. Incorporating model complexity and spatial sampling bias into ecological niche models of climate change risks faced by 90 California vertebrate species of concern. *Diversity and Distributions* 20: 334–343.
- Westerling, A.L., H.G. Hidalgo, D.R. Cayan, and T.W. Swetnam. 2006. Warming and earlier spring increases western US forest wildfire activity. *Science* 313: 940–943.
- Wotton, B.M. and D.L. Martell. 2005. A lightning fire occurrence model for Ontario. *Canadian Journal of Forest Research* 35: 1389-1401.
- Wisz, M.S., R.J. Hijmans, J. Li,, A.T. Peterson, C.H. Graham, A. Guisan, NCEAS Predicting Species Distributions Working Group. 2008. Effects of sample size on the performance of species distribution models. *Diversity and Distributions* 14: 763-773.
- Yiwen, Z., B.W. Low, and D.C.J. Yeo. 2016. Novel methods to select environmental variables in MaxEnt: A case study using invasive crayfish, *Ecological Modelling* 341: 5-13.

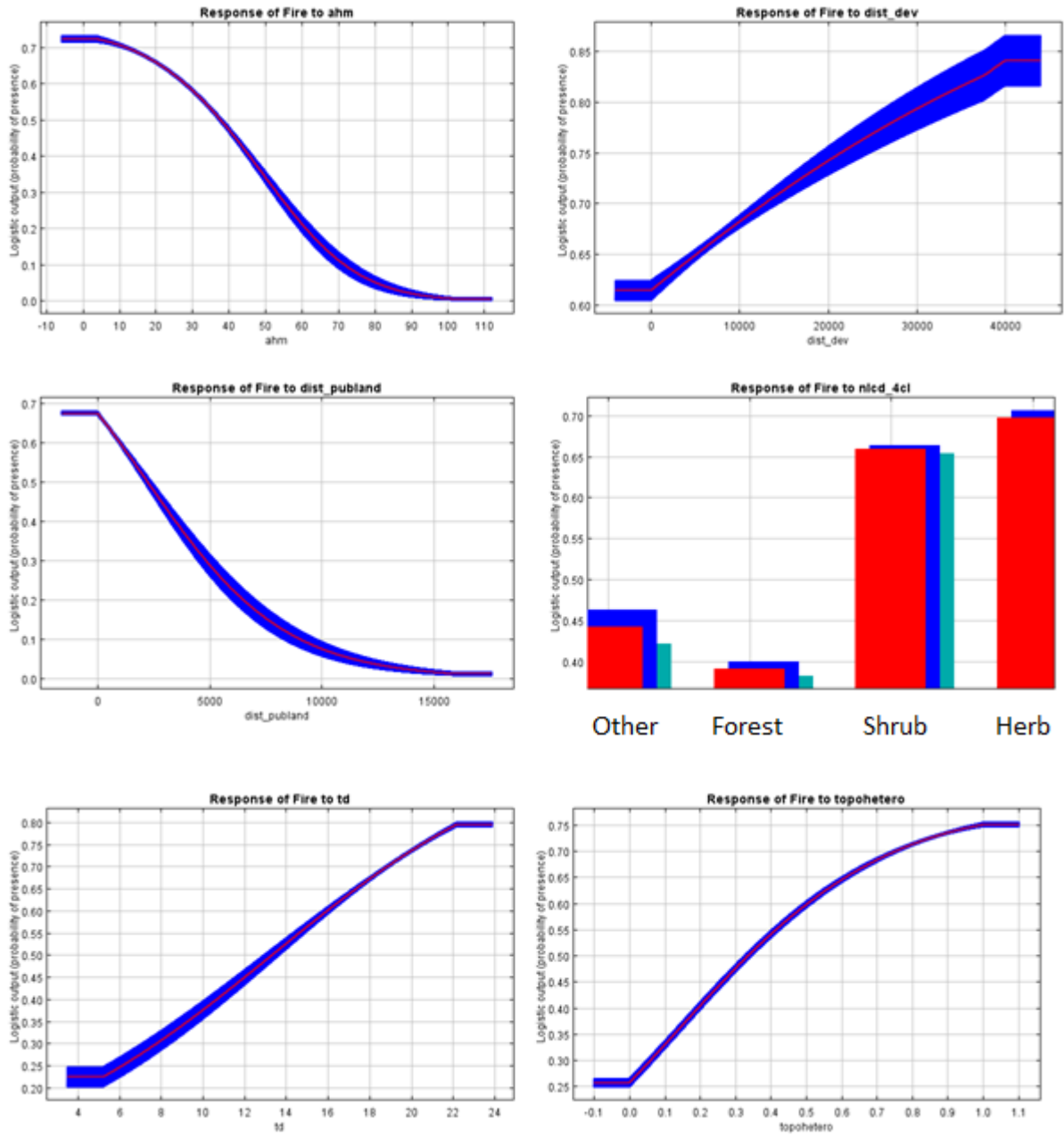


**Appendix 2. Model response plots**

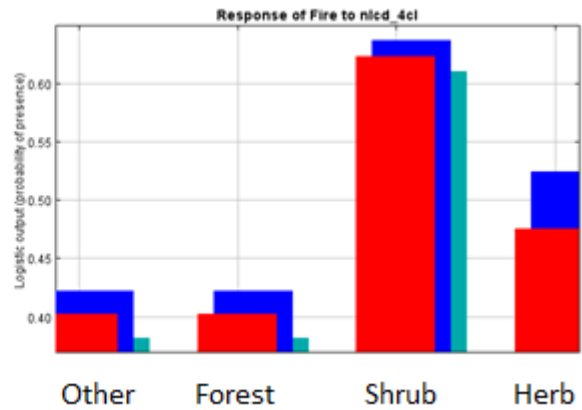
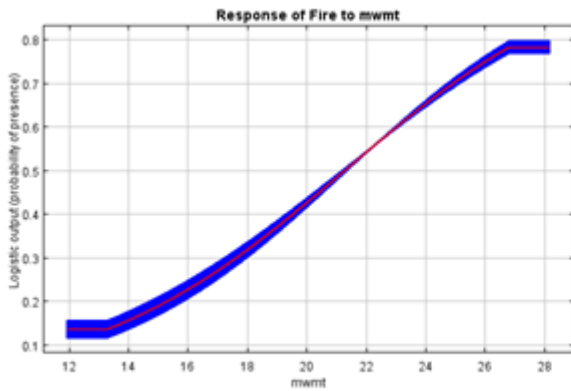
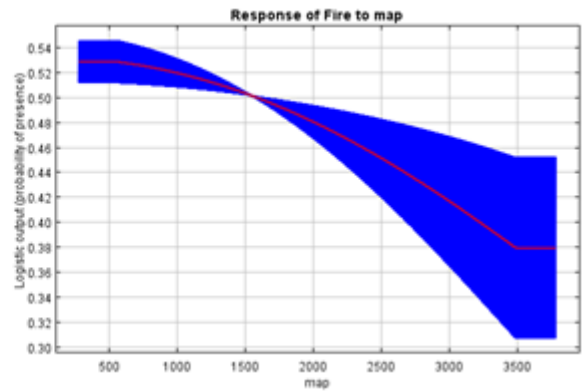
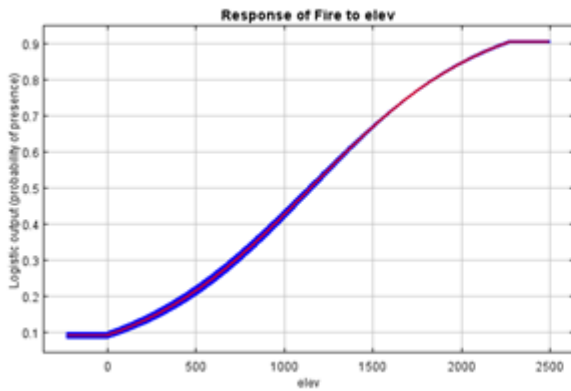
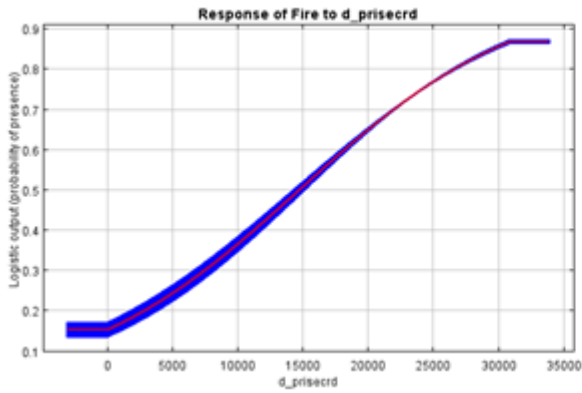
- A. Region-wide model
  - a. Univariate plots

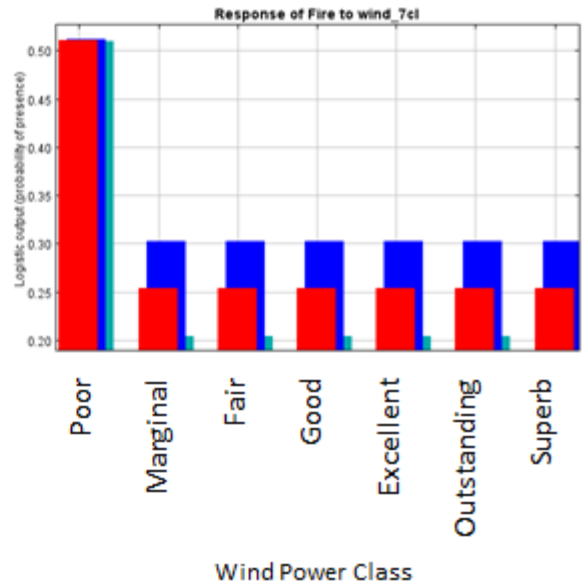
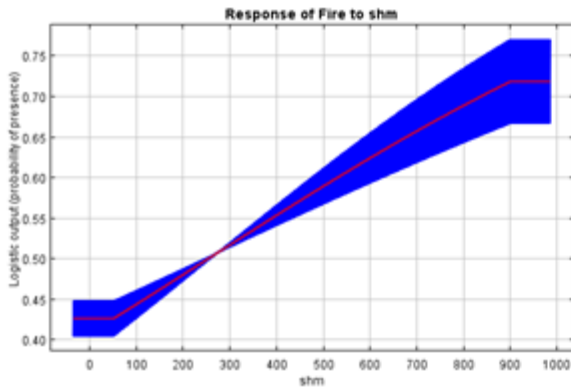


- b. Marginal plots

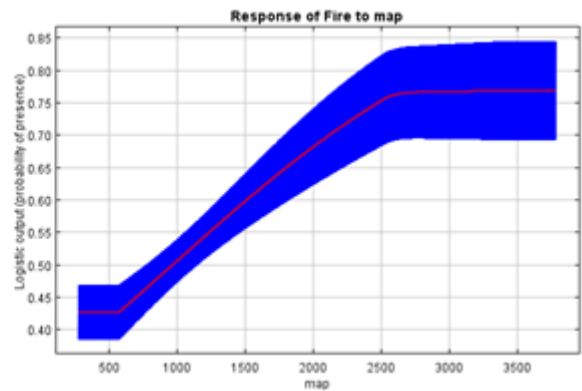
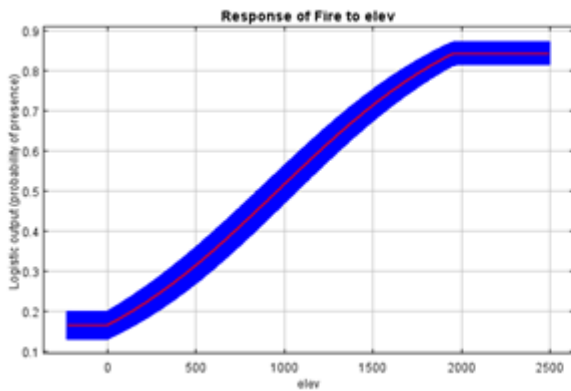
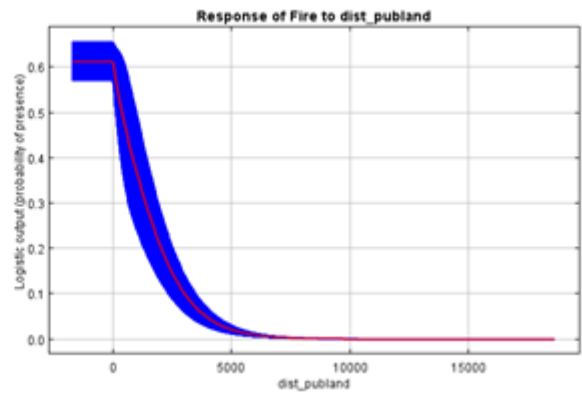
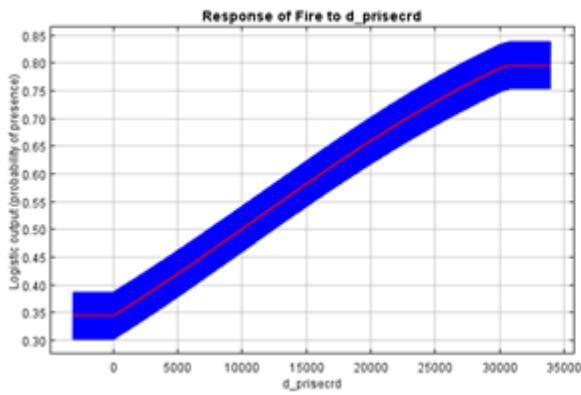


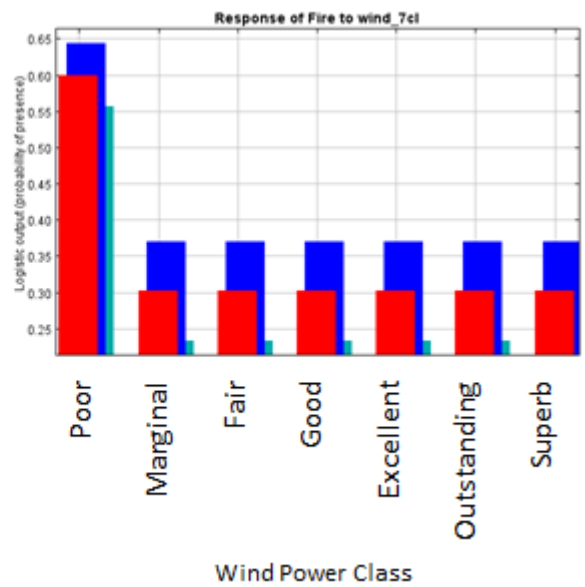
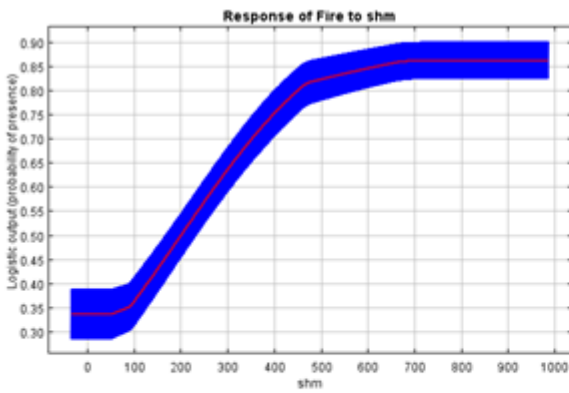
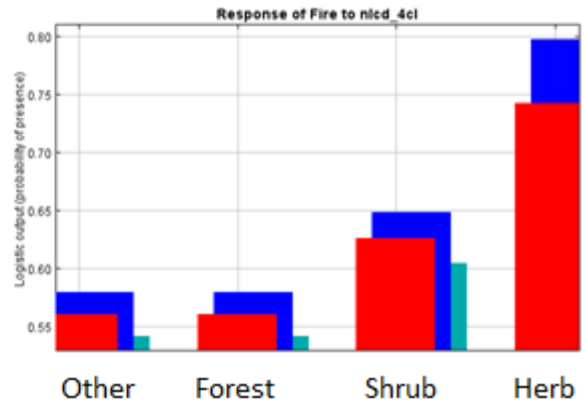
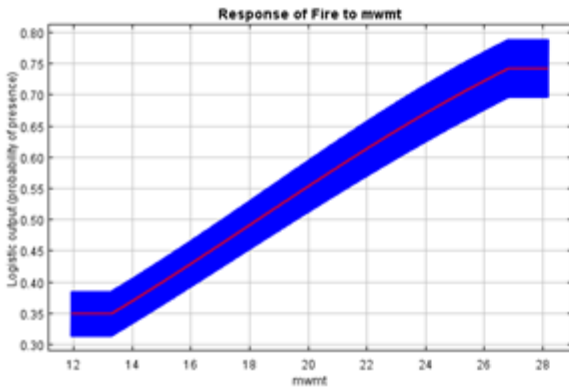
B. Subregion 1a model  
 a. Univariate plots



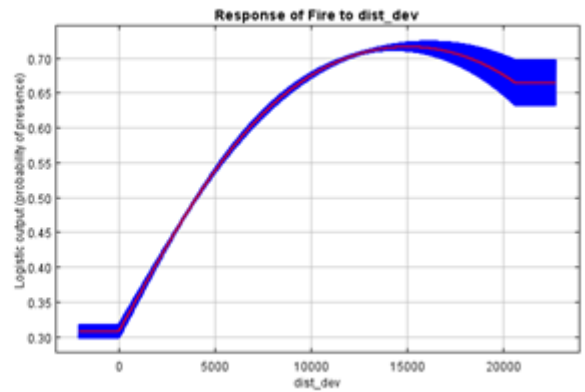
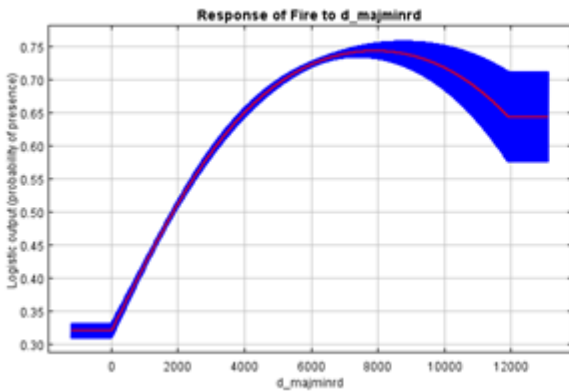


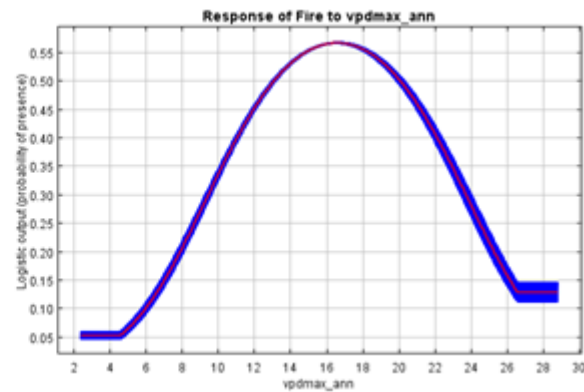
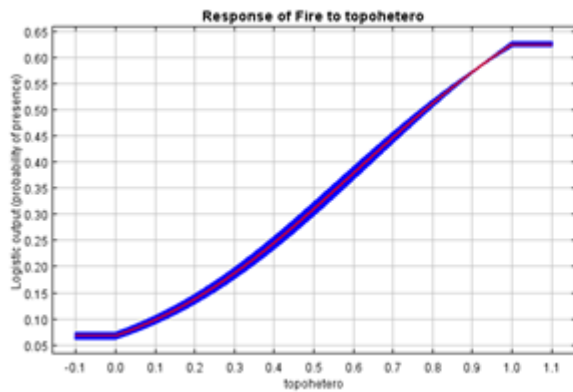
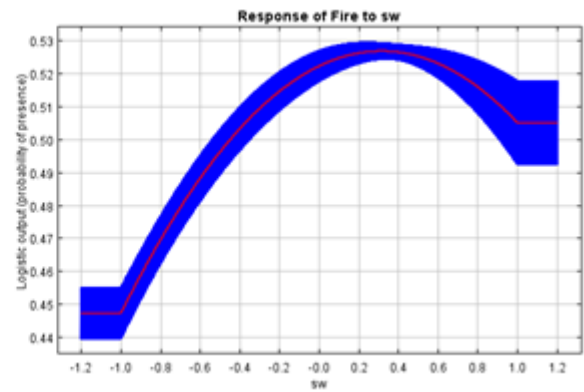
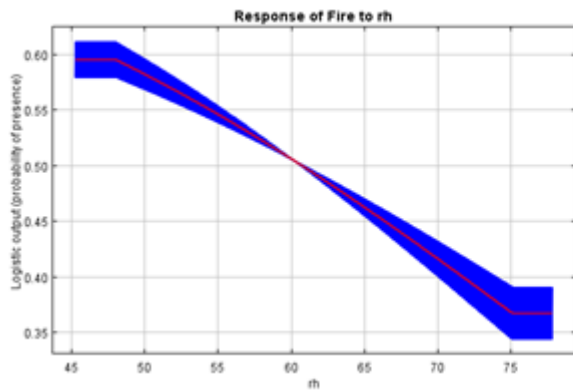
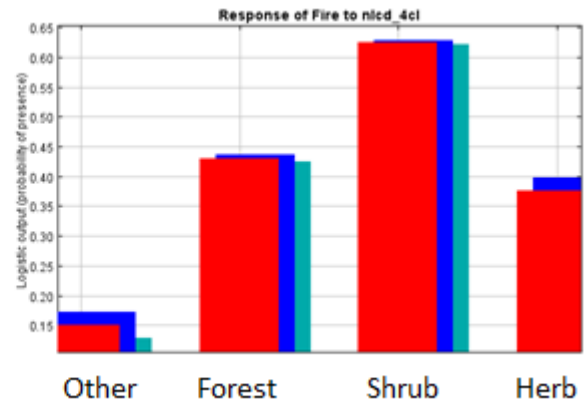
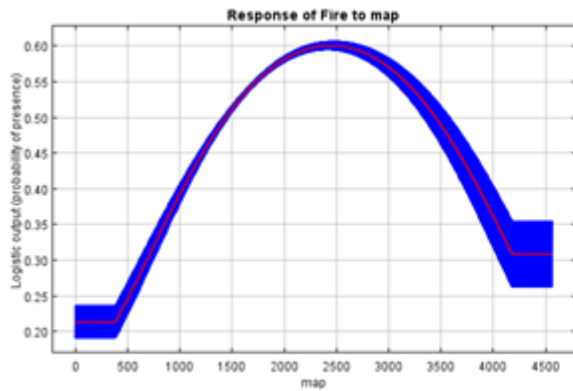
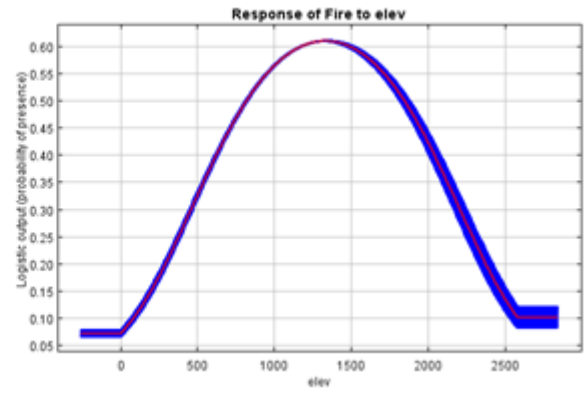
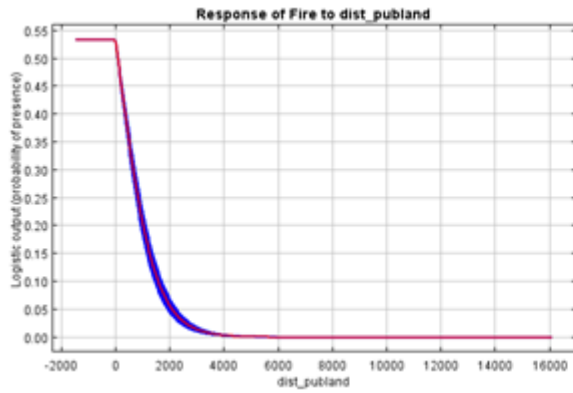
b. Marginal plots



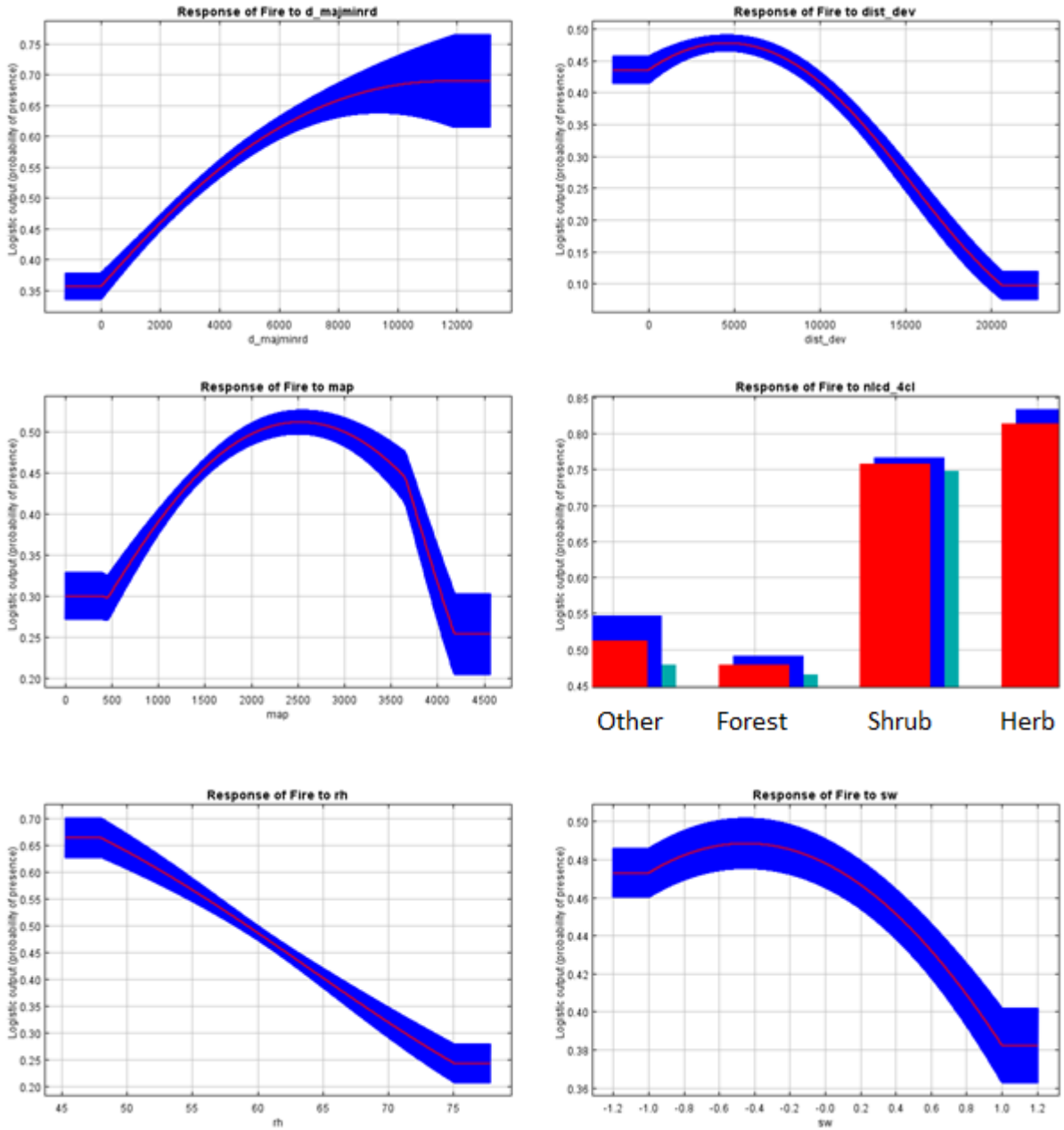


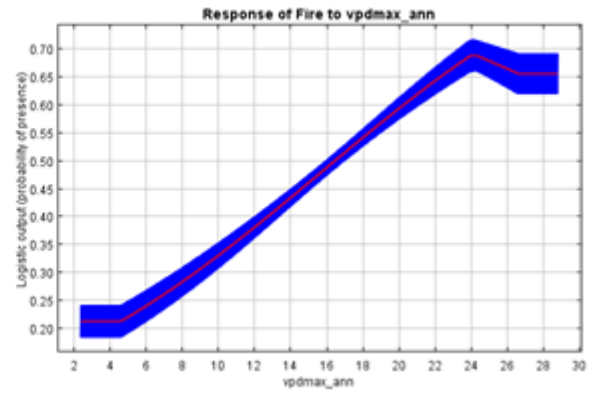
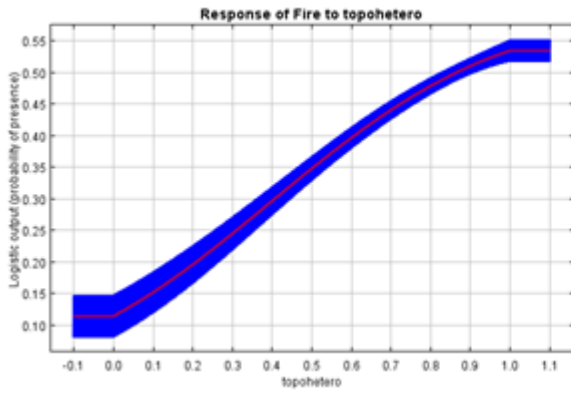
C. Subregion 1b model  
a. Univariate plots



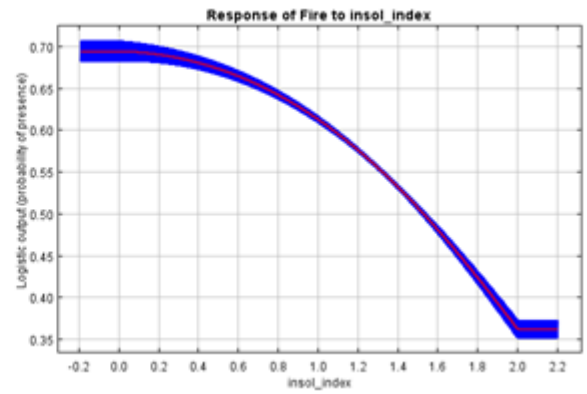
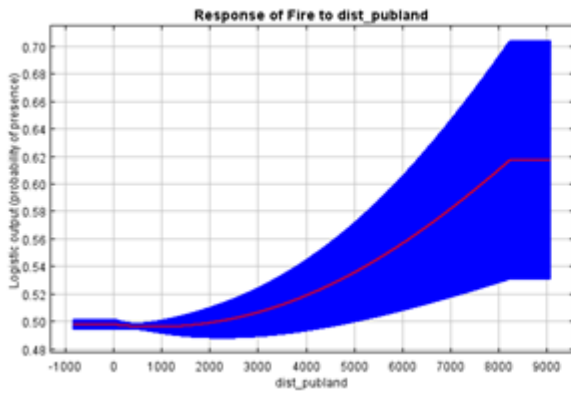
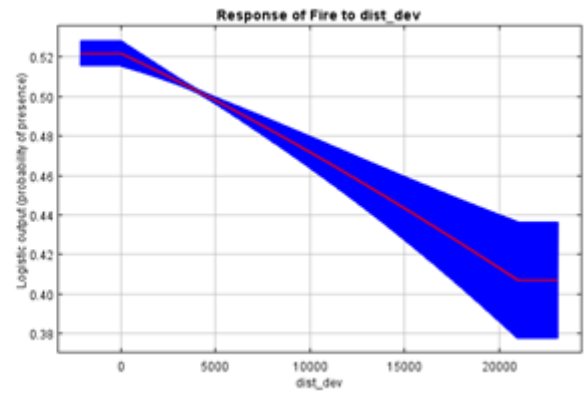
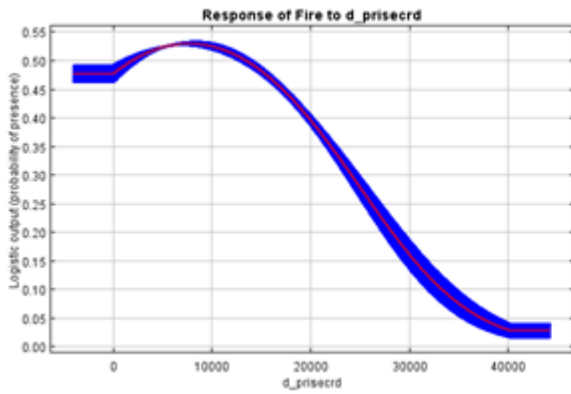


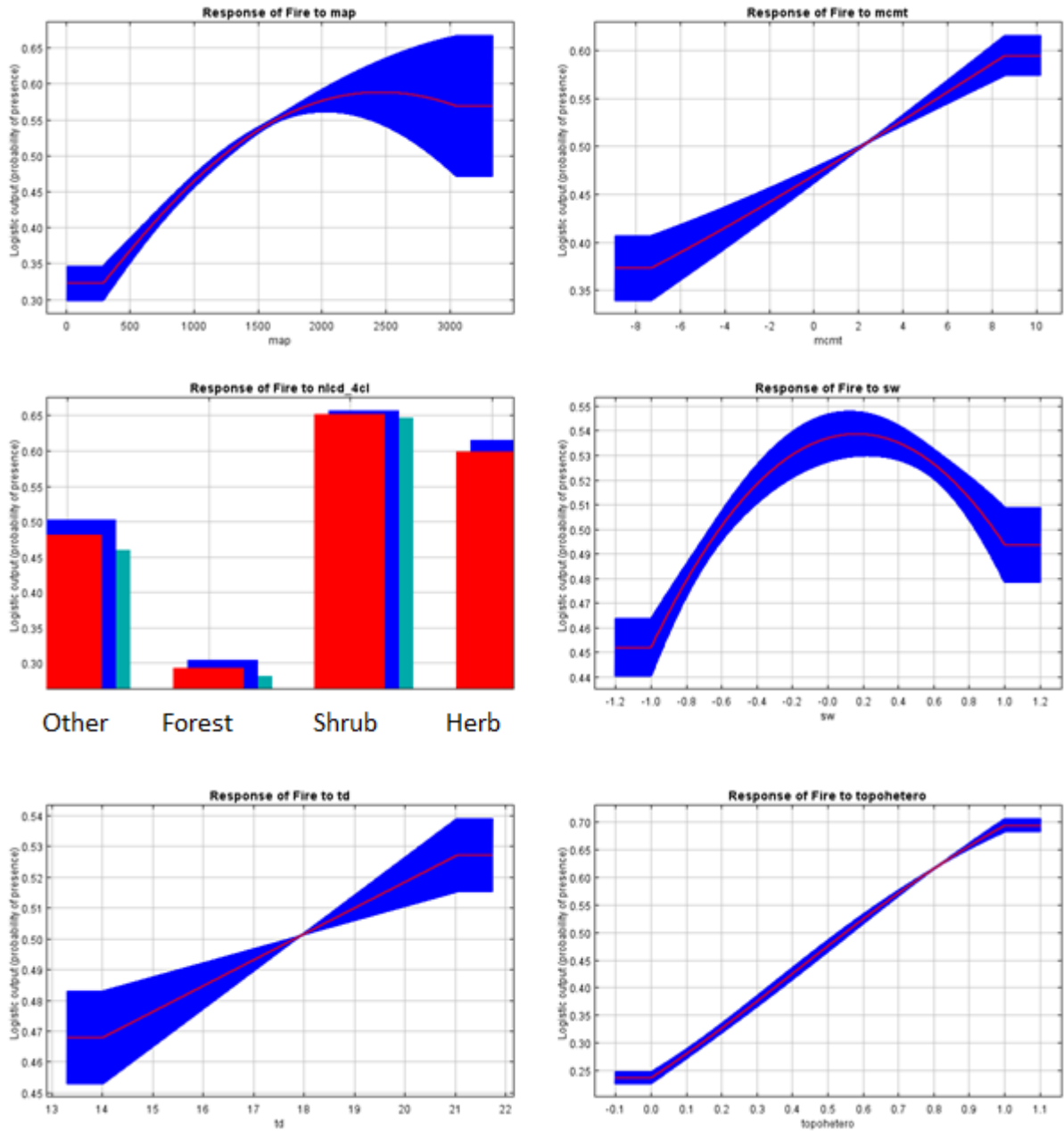
b. Marginal plots



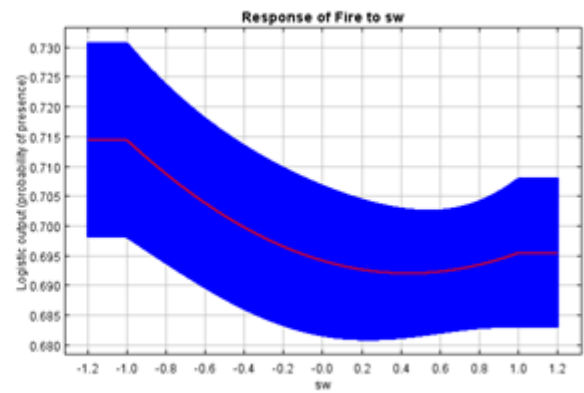
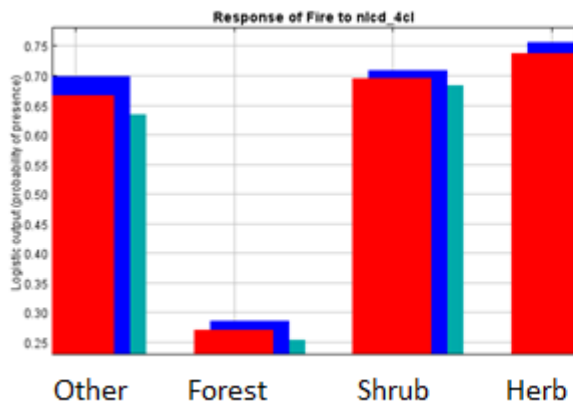
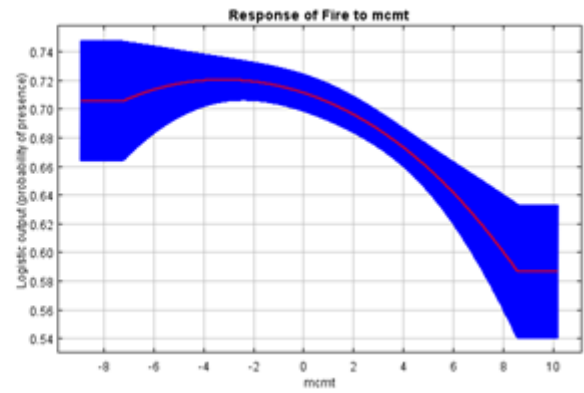
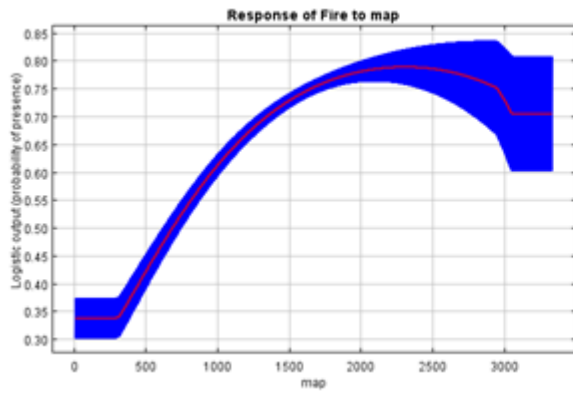
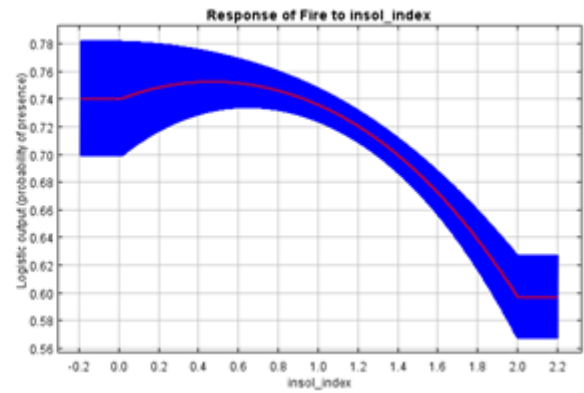
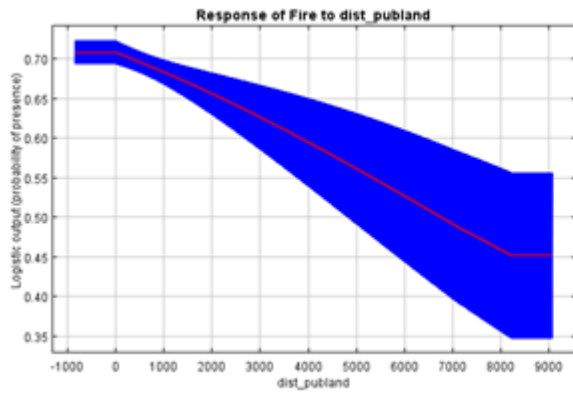
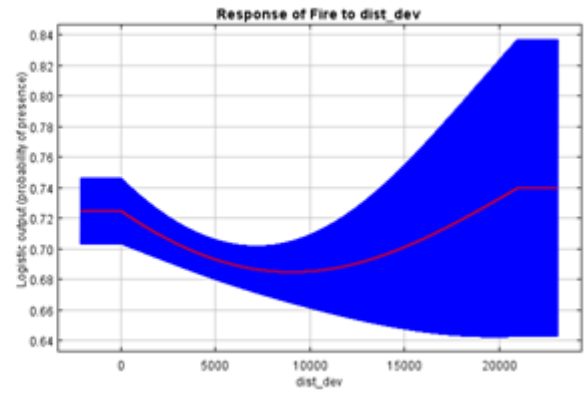
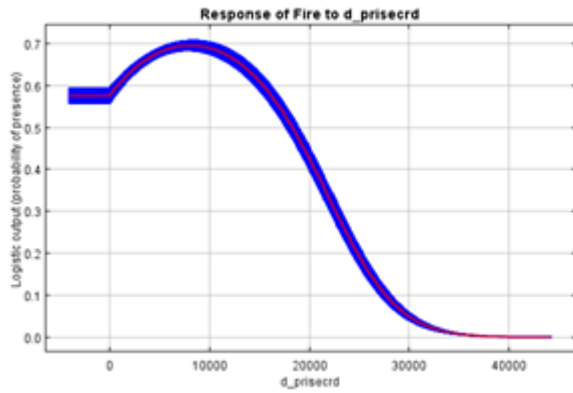


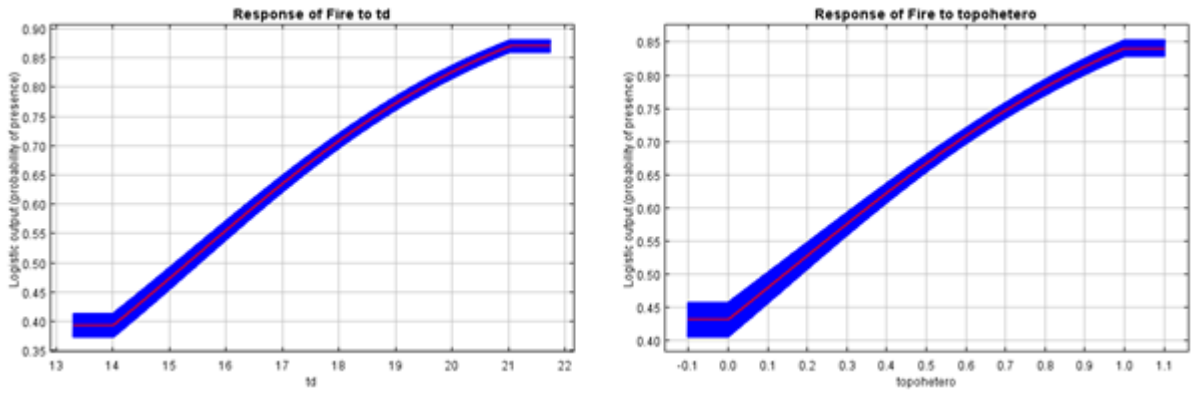
D. Subregion 2 model  
a. Univariate plots



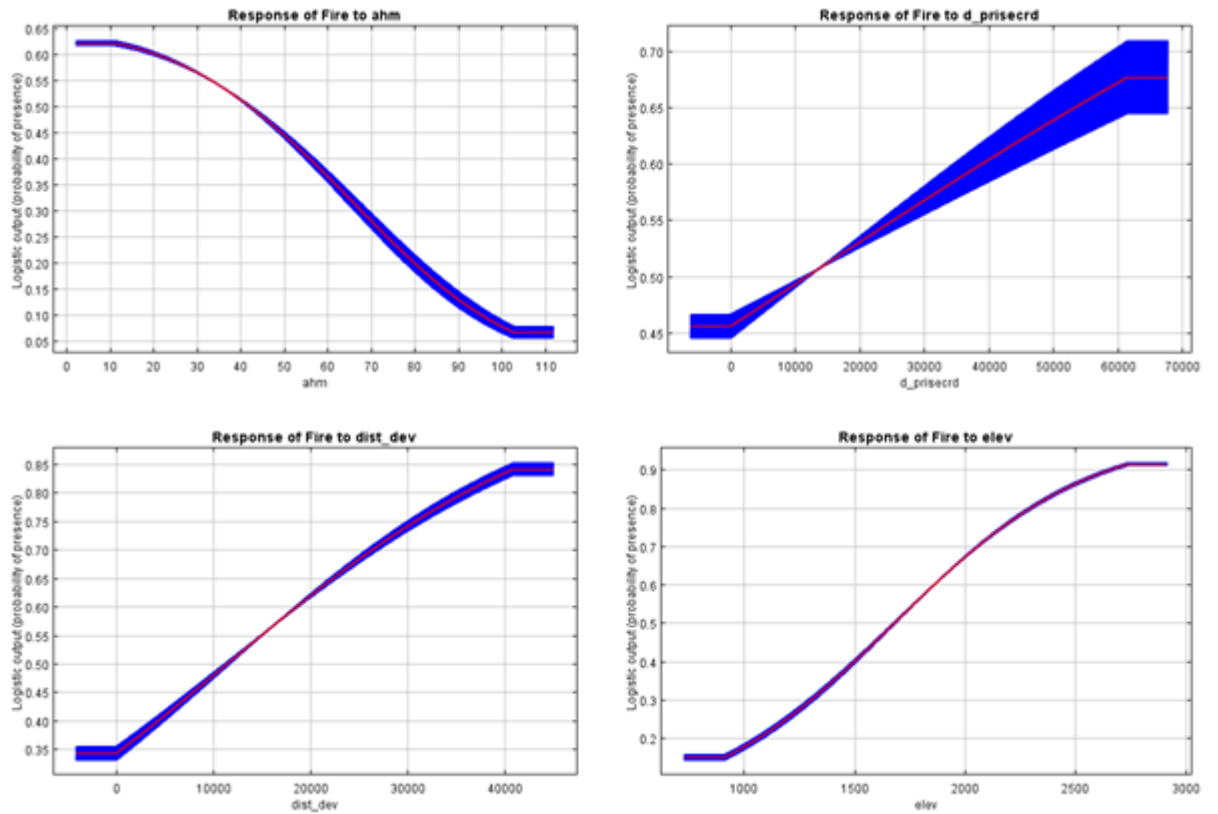


b. Marginal plots

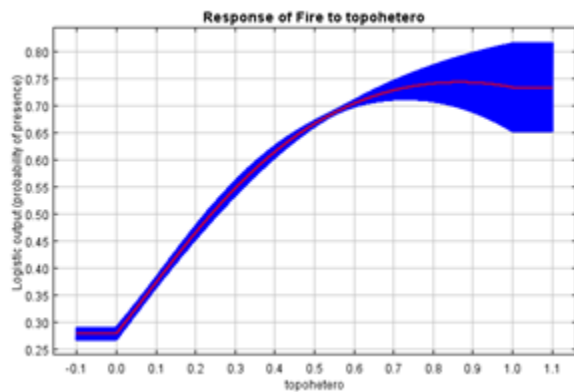
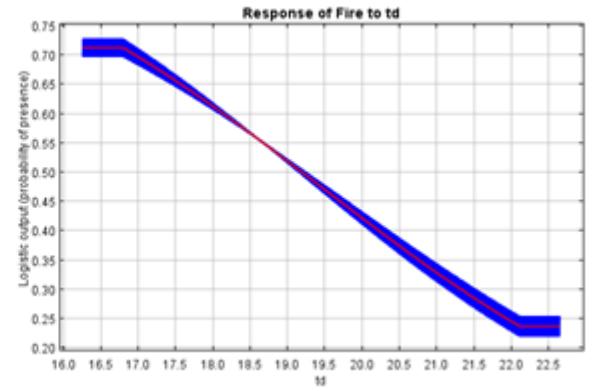
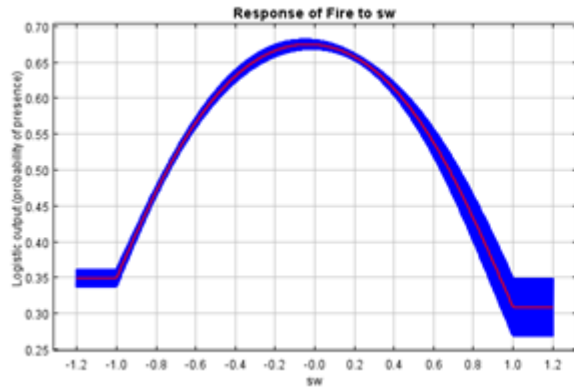
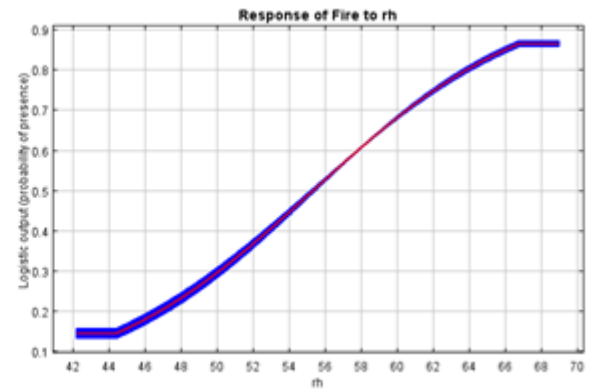
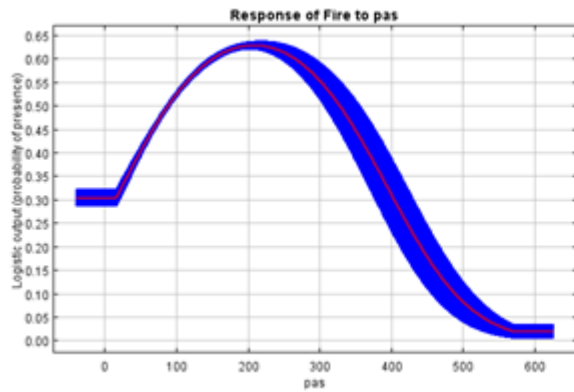
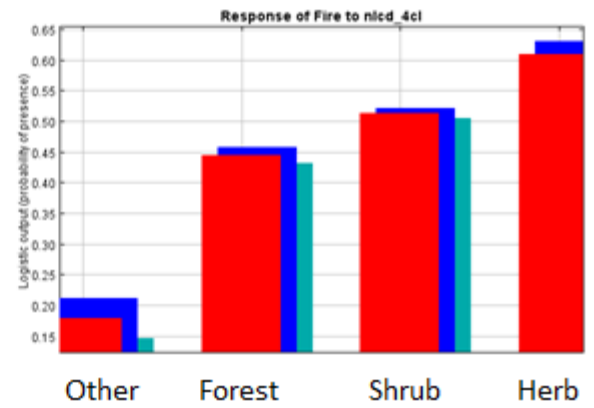
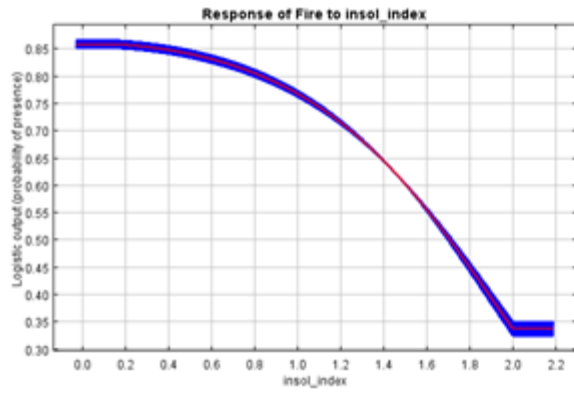




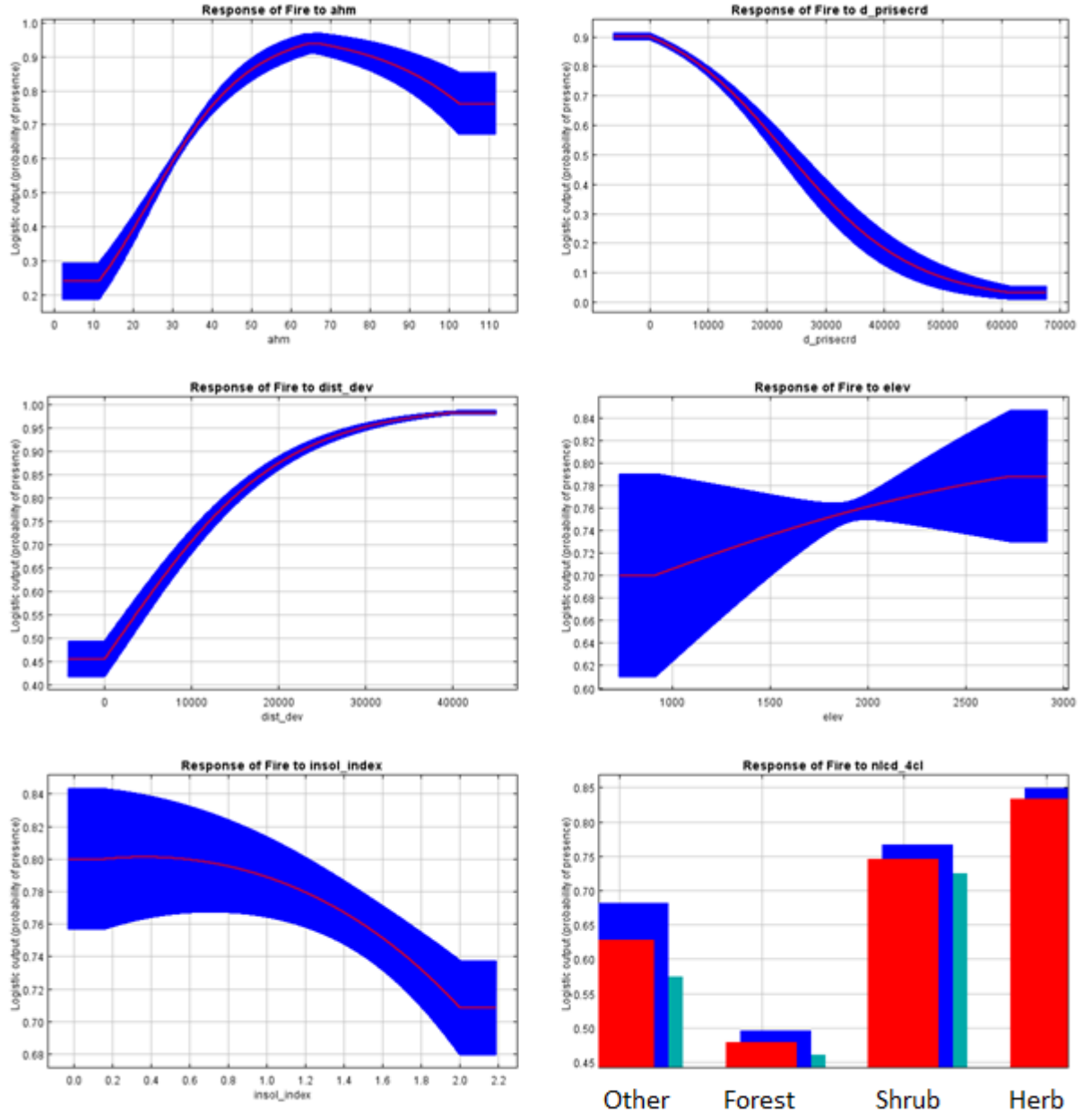
E. Subregion 3 model  
a. Univariate plots



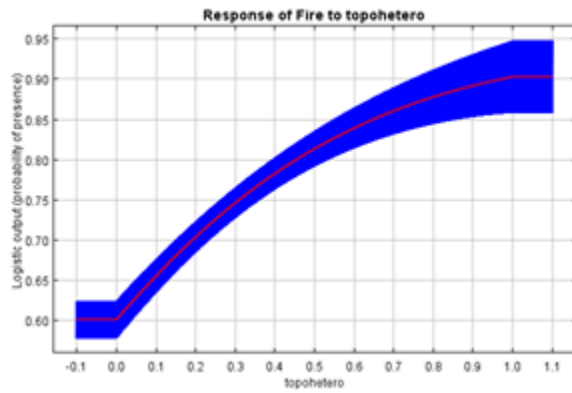
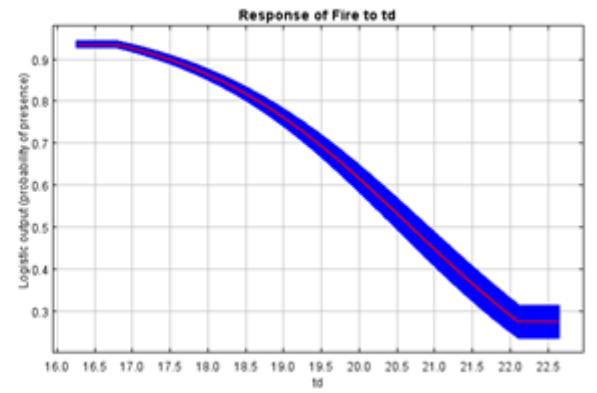
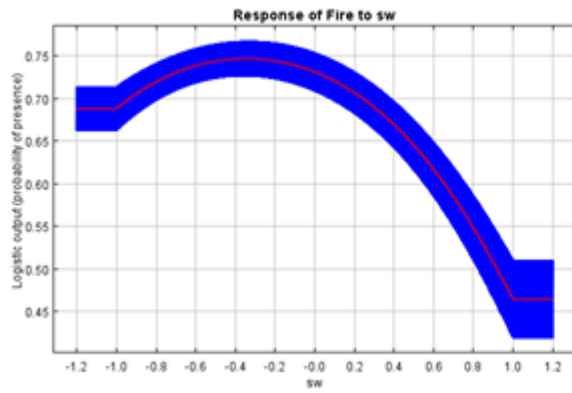
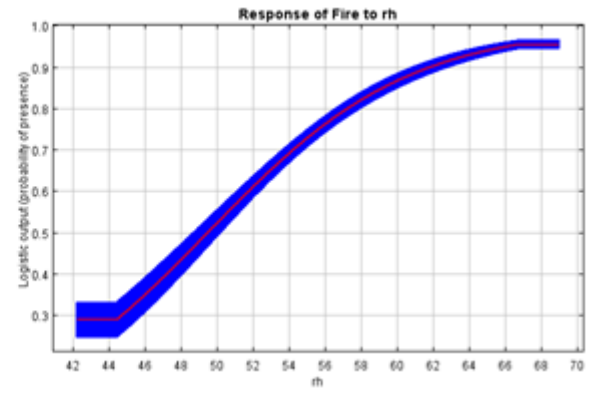
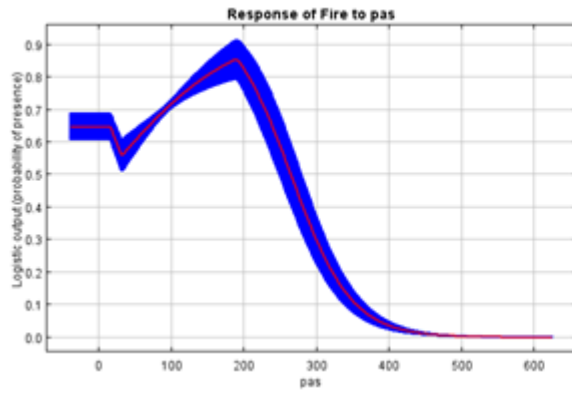
Modeling the Potential for Large High-Severity Fires in the Klamath Basin Region of California and Oregon and Their Potential Impacts on Marten and Fisher Conservation Biology Institute, September 2019



b. Marginal plots



Modeling the Potential for Large High-Severity Fires in the Klamath Basin Region of California and Oregon and Their Potential Impacts on Marten and Fisher Conservation Biology Institute, September 2019



Appendix 3. Black and white versions of figures.

Figure 1.

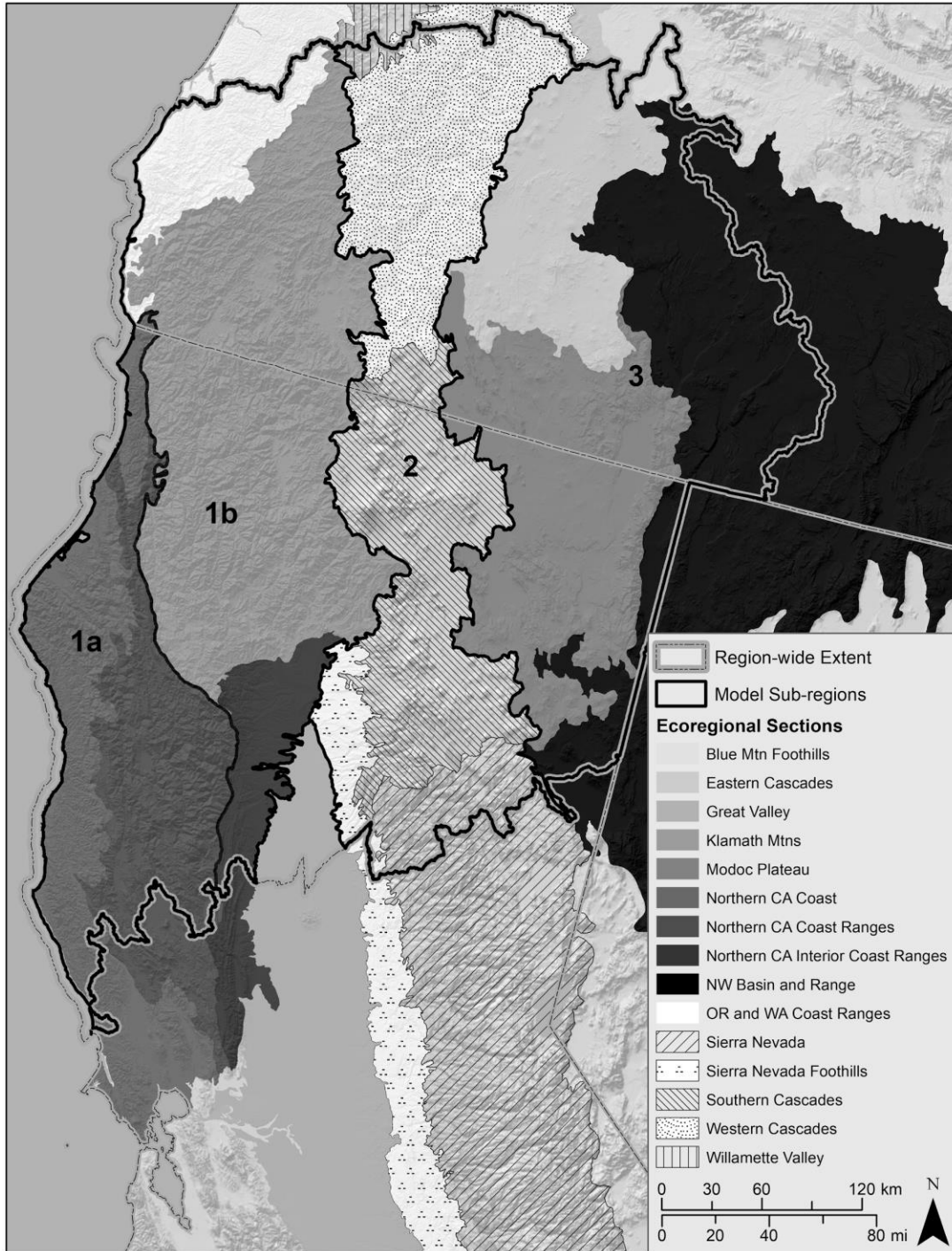


Figure 2.

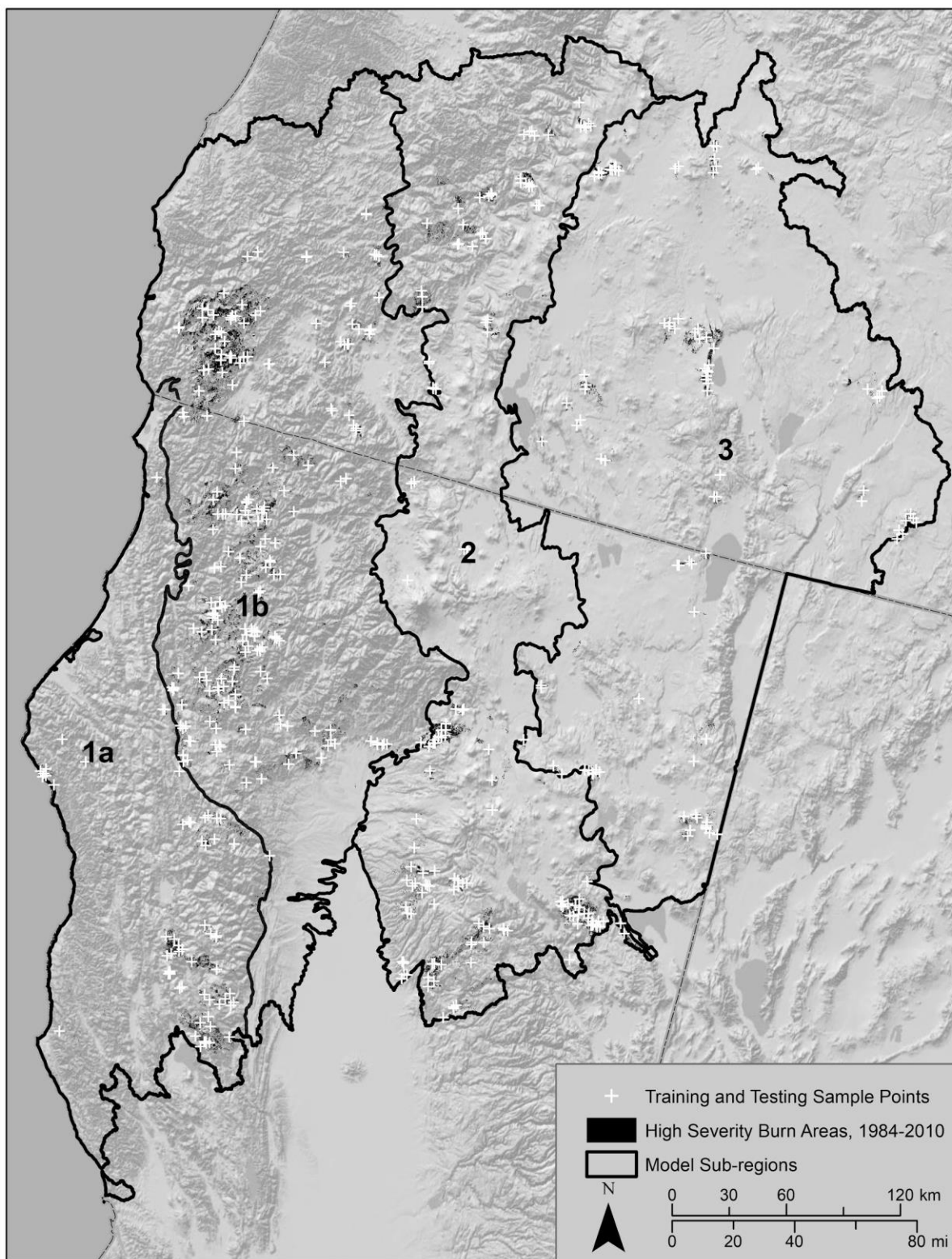


Figure 3.

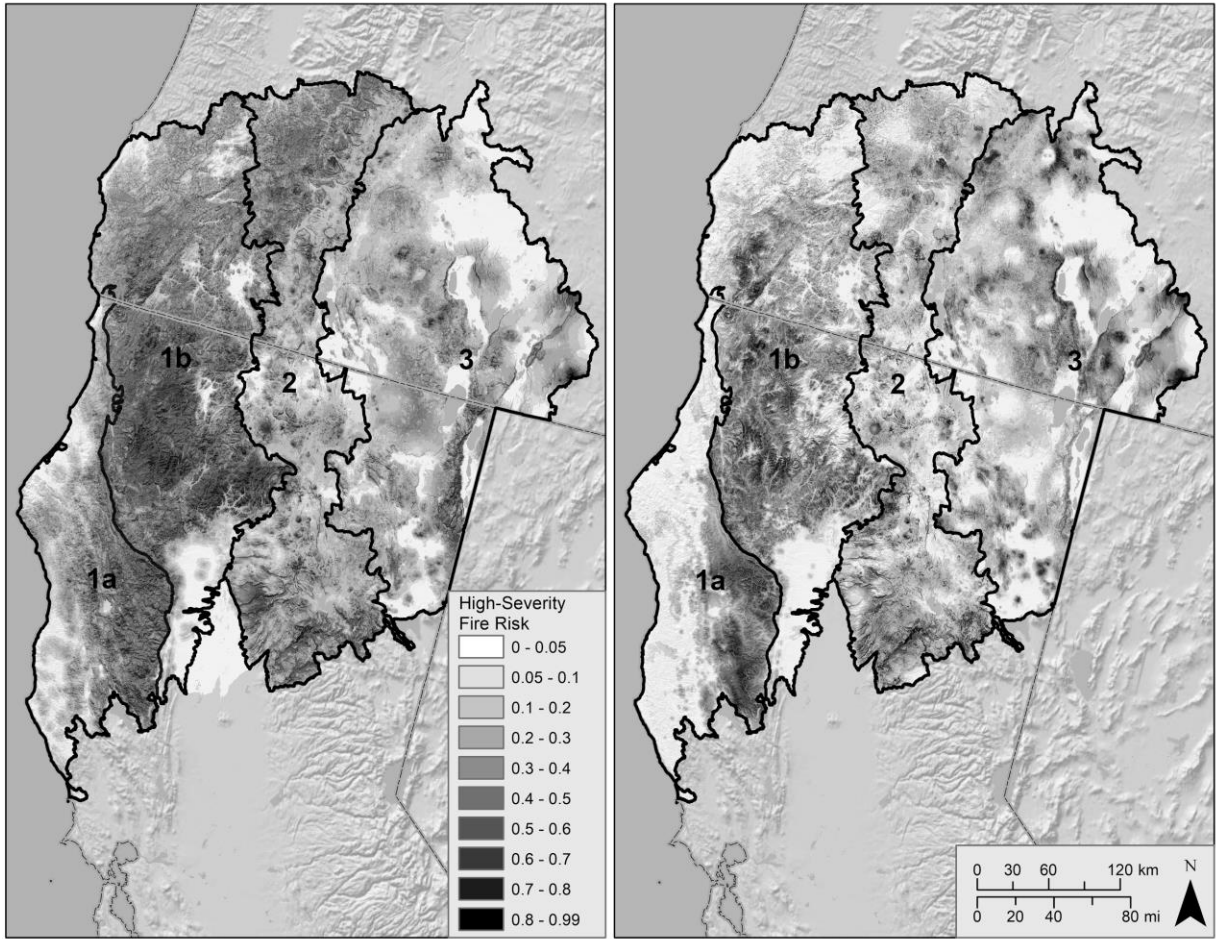


Figure 4.

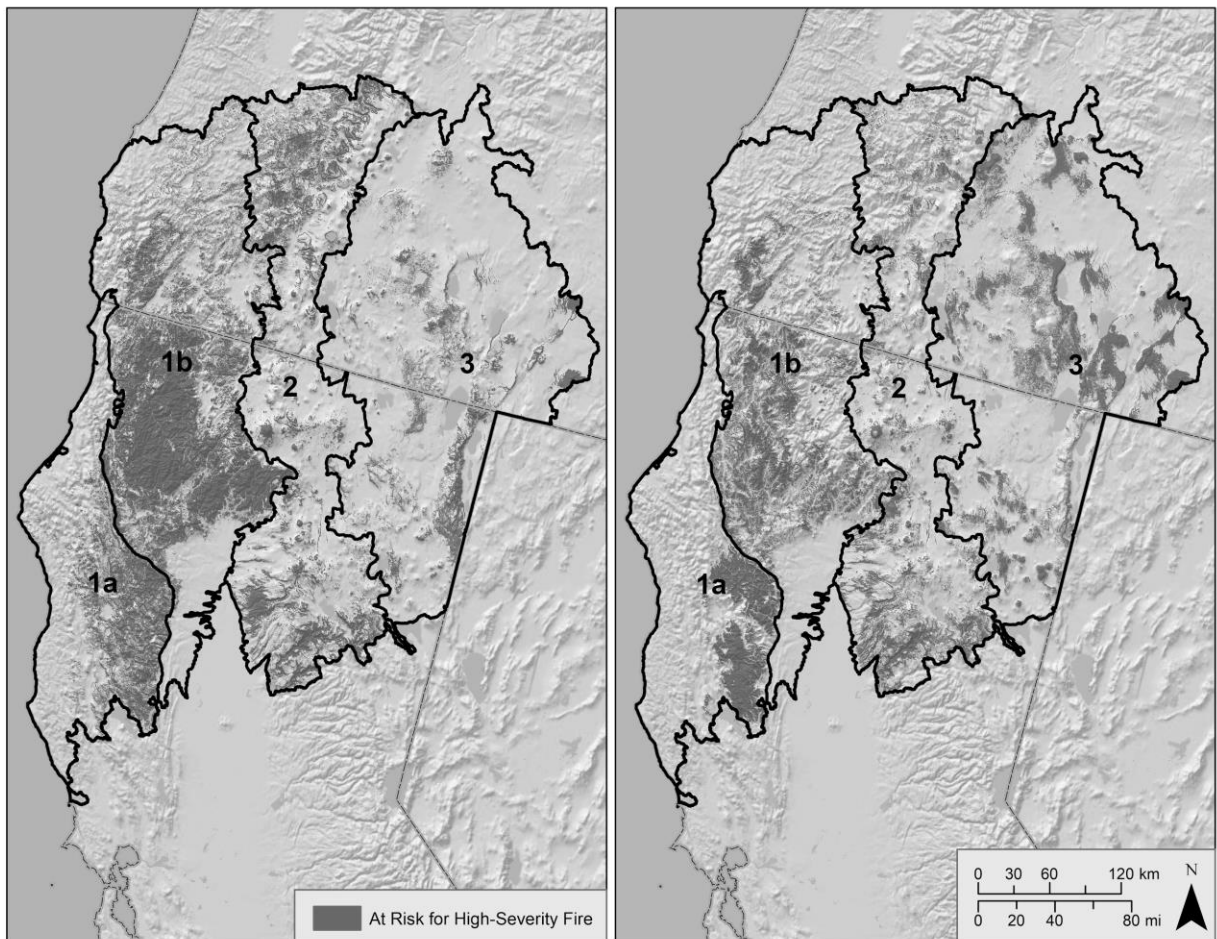


Figure 5.

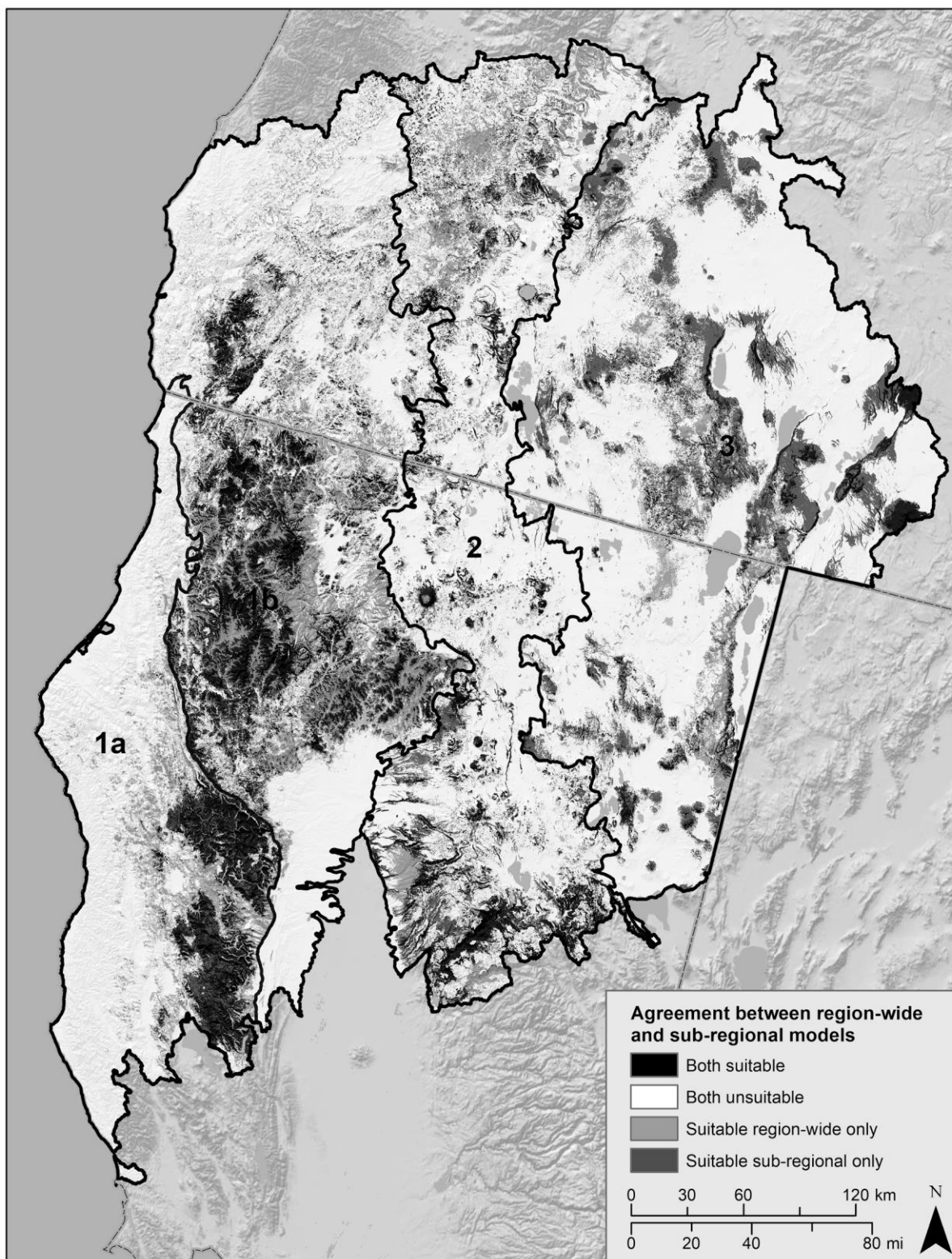


Figure 6.

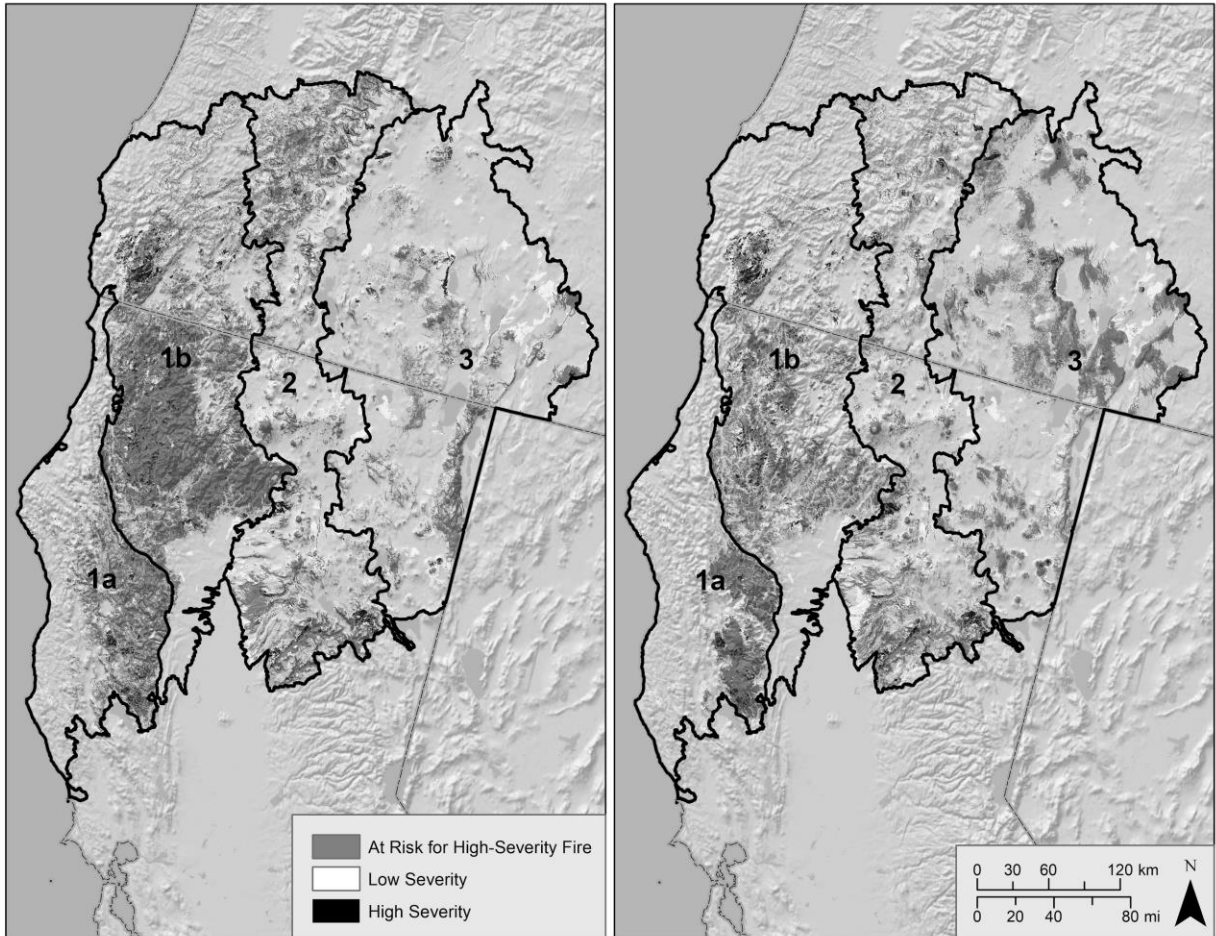


Figure 7.

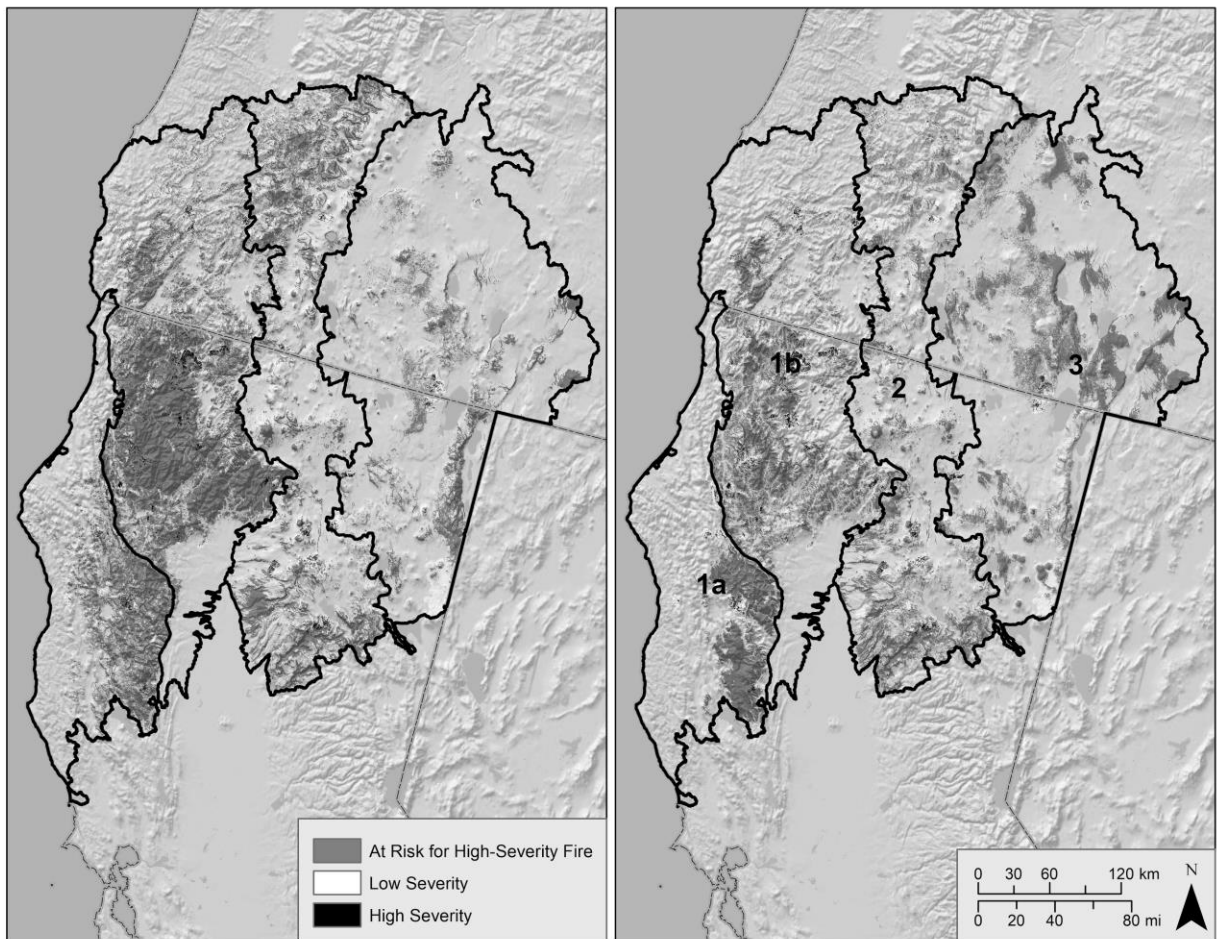


Figure 8.

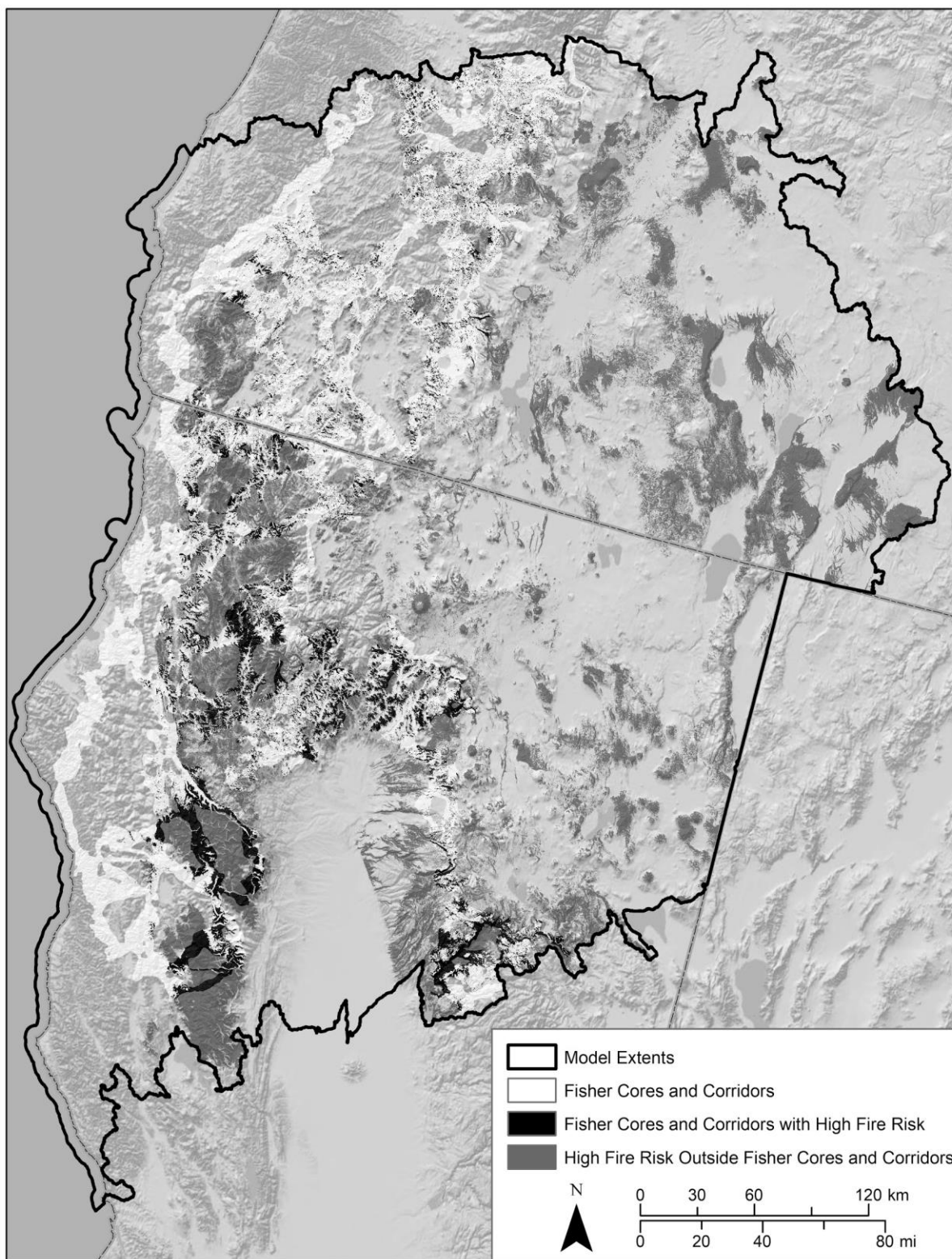


Figure 9.

